

Tracer-based analysis of spatial and temporal variation of water sources in a glacierized catchment

Short title:

Tracer-based analysis of water sources

Daniele Penna^{1,2,3}, Michael Engel^{21,42}, Luca Mao⁵³, Andrea Dell'Agnese²¹, Giacomo Bertoldi⁴²,
Francesco Comiti²¹

~~¹Department of Environment Sciences System, Swiss Federal University of Technology (ETH),
Universitätstrasse 16, CH-8092, Zurich, Switzerland.~~

²¹Faculty of Science and Technology, Free University of Bozen-Bolzano, piazza Università 5, 39100,
Bolzano, Italy

~~³Department of Land, Environments, Agriculture and Forestry, University of Padova, viale
dell'Università 16, 35020 Legnaro (PD), Italy.~~

⁴²Institute for Alpine Environment, EURAC, viale Druso 1, Bozen-Bolzano, Italy

⁵³Department of Ecosystems and Environment, Pontificia Universidad Católica de Chile, Av. Vicuña
Mackenna 4860, Macul, Casilla 306-22, Santiago, Chile

Correspondence to:

Daniele Penna,

¹Faculty of Science and Technology, Free University of Bozen-Bolzano, piazza Università 5, 39100,
Bolzano, Italy

~~Department of Environment Sciences System, Swiss Federal University of Technology (ETH),
Universitätstrasse 16, CH-8092, Zurich, Switzerland.~~

Email: daniele.penna@ethz.unibz.ch

~~ph.: +41 44 6338197~~

Submitted for publication in Hydrology and Earth System Sciences

April 2014

Formatted: Don't adjust space between Latin and Asian text, Don't adjust space between Asian text and numbers

Formatted: English (United Kingdom)

Abstract

Snow-dominated and glacierized catchments are important sources of fresh water for biological communities and for population living in mountain valleys. Gaining a better understanding of the runoff origin and of the hydrological interactions between meltwater and streamflow is critical for natural risk assessment and mitigation as well as for effective water resources management in mountain regions. This study is based on the use of stable isotopes of water and electrical conductivity as tracers to identify the water sources for runoff and their seasonal variability in a glacierized catchment in the Italian Alps. Samples were collected from rainfall, snow, snowmelt, ice melt and stream water (from the main stream at different locations and from selected tributaries) in 2011, 2012 and 2013. The tracer-based mixing analysis revealed that, overall, snowmelt and glacier melt were the most important end-members for stream runoff during late spring, summer and early fall. The temporal variability of the tracer concentration suggested that stream water was dominated by snowmelt at the beginning of the melting season (May-June), by a mixture of snowmelt and glacier melt during mid-summer (July-early August), and by glacier melt during the end of the summer (end of August-September). The same seasonal pattern observed in streamflow was also evident for groundwater, with the highest electrical conductivity and least negative isotopic values found during periods of limited melting. Particularly, the application of a two-component mixing model to data from different springs showed that the ~~overall~~ snowmelt contribution to groundwater recharge varied between 21% ($\pm 3\%$) and 93% ($\pm 1\%$) over the season, and the overall contribution during the three study years ranged between 58% (± 24 ~~15~~%) and 72% ($\pm 15~~19~~%). These results provided new insights on the isotopic characterization of the study catchment and the presented approach could offer further understanding of the spatio-temporal variability of the main water sources contributing to runoff in other snow-dominated and glacierized Alpine catchments.$

1. Introduction

High-elevation mountain catchments are environments of highly economic and social value since they store large volumes of water in form of snow and ~~glacier ice~~ bodies and release it on a seasonal basis as meltwater. Large populations living downstream of glacierized catchments primary rely on snow and glacier meltwater for drinking and irrigation needs (Kriegel et al., 2013). Meltwater plays also an important role in the aquatic ecology of downstream reaches, because it regulates summer stream temperatures, maintaining high-quality habitat for fish and cold-water communities (Grah and Beaulieu, 2013). From a hydrological perspective, snowmelt and glacier melt are important because moderate inter-annual variability in streamflow (Stewart, 2009), and can maintain elevated discharge during the dry season or relatively dry years (Milner et al., 2009) when water demand is highest.

66

67 High-elevation catchments are complex environmental systems where different water sources interact
68 to affect the streamflow regime and the geochemical composition of stream water. Understanding
69 such a complexity is a first step towards a better conceptualization of catchment functioning that is
70 ~~critical-essential~~ for natural risk assessment and mitigation as well as for effective water resources
71 management in mountain regions. This is even more critical under the current changing climatic
72 conditions, to which snow-dominated and glacierized environments are particularly vulnerable. ~~Thus,~~
73 ~~the~~ expected future retreat of mountain glaciers and earlier melt of snowpack is producing marked
74 effects on the water balance. In future, mean annual runoff is expected to decrease but peak runoff is
75 likely to increase (Molini et al., 2011), with seasonal shifts in the runoff regime (Kääb et al., 2007)
76 and in the relative timing and contribution of the different water sources ~~on-to~~ baseflow, peak flow
77 and groundwater. This raises major concerns about water supply security in mountain regions
78 (Uhlmann et al., 2013).

79

80 ~~In this context, order to better predict the future hydrological behaviour in such rapidly changing~~
81 ~~environments~~ there is an urgent need to obtain a more detailed understanding ~~of runoff origin and of~~
82 ~~the dynamic interactions between meltwater and streamflow~~ hydrological processes and of runoff
83 ~~origin~~ in glacierized catchments, ~~in order to better predict the future hydrological behaviour in such~~
84 ~~rapidly changing environments. This would allow developing a broader view encompassing the~~
85 ~~dynamic interactions between meltwater and streamflow to eventually conceptualize the catchment~~
86 ~~internal hydrological functioning.~~ For this purpose, a powerful investigation tool is represented by
87 tracers. Particularly, the stable isotopes of water ($\delta^2\text{H}$ and $\delta^{18}\text{O}$) have been recently used in high-
88 elevation catchments to quantify post-snowmelt summer rainfall contributions to streamflow (Dahlke
89 et al., 2013), estimate the regional water balance (Ohlanders et al., 2013), compute catchment
90 residence times (Jeelani et al., 2013; Chiogna et al., 2014) and constrain model parameters (Cable et
91 al., 2011). Moreover, water isotopes, coupled to other geochemical tracers, such as electrical
92 conductivity (EC), have the potential to identify end-members (i.e., the dominant sources to runoff)
93 and compute their contribution to streamflow (Maurya et al., 2011).

94

95 The discharge due to snow and glacier meltwater during spring and summer is relevant for the yearly
96 runoff regime of streams in high-elevation Alpine areas (Koboltschnig and Schöner, 2011).
97 Particularly, inner valleys of the Alps are characterized by relatively low amounts of liquid
98 precipitation and significantly benefit from the water contribution provided by lateral valleys where
99 snowmelt and/or glacier melt dominate streamflow. One clear example is given by the

Vinschgau/Venosta valley, in South Tyrol (Eastern Italian Alps), ~~where most of the economy is based on. The primary voice in the economy of population living there is~~ the cultivation of apples. Since ~~here~~ the climate is relatively dry (the mean annual precipitation for the period 1989–2012 in Laas-Lasa, at 863 m a.s.l. was 480 mm) a large part of water supply derives from stream water from the tributaries of the main valley, which are used for pressurized irrigation and hydropower production. Given the socio-economic importance of meltwater in this region, we conducted an experimental research in the glacierized Saldur catchment, one of the catchment that contributes to water availability in the upper Vinschgau valley. Importantly, the glacier in the Saldur catchment is melting at a particularly fast rate, with 20% of areal reduction from 2005 to 2013 (Galos and Kaser, 2014). The Saldur catchment has been recently objective of different hydrological studies (e.g., Bertoldi et al., 2014; Della Chiesa et al., 2014; Pasolli et al., 2014) but an assessment of the runoff water sources and of their spatio-temporal variability ~~along with~~ based on an isotopic characterization of the catchment is still ~~missing~~ lacking.

In this paper, we take advantage of the combined use of two tracers, namely stable isotopes of water and EC, sampled from precipitation and different water bodies ~~of over~~ three consecutive years, to:

- i) define the origin of vapour masses that form precipitation in the study area;
- ii) identify the end-members to streamflow;
- iii) understand the seasonal variability of ~~snowmelt and ice melt contribution to tracer concentration in runoff~~ stream water and groundwater;
- iv) quantify the role of snowmelt on groundwater recharge.

2. Study Area

The field activities were carried out in the upper Saldur/Saldura catchment (61.7 km²) ~~lying located~~ in the upper Vinschgau/Venosta valley, South Tyrol (Eastern Italian Alps). Elevations in the catchment range from 1.632 m a.s.l. at the outlet—chosen at a gauging station upstream of the confluence with the Etsch/Adige River—to 3.725 m a.s.l. of the highest peak (Weißkugel/Palla Bianca). The upper part of the catchment hosts the Matsch/Mazia glacier (extent of 2.2 km² in 2013, Galos and Kaser, 2014) whose current snout lies approximately at 2800 m a.s.l. and feeds the Saldur River. Downstream of the glacier snout, the Saldur River receives water contributions from various tributaries, most of them, especially on the left side of the valley, originating at elevations above 2900 m a.s.l. and therefore ~~seasonally snow-covered~~ approximately from October/November to May/June by snow. As such, streamflow during summer and part of spring and fall is noticeably affected by water inputs mainly deriving from melting of the glacier body and ~~of~~ the winter snowpack

134 in different portions of the catchment. Glacier erosion formed the typical U-shape in the upper valley
135 that is partly filled with sediment from talus, small shallow landslides and large alluvial/debris fans
136 from the steep tributaries. The average slope of the catchment is 31.8° and the aspect is predominantly
137 towards South (Fig. 1 and Table 1).
138

139 The study area has a continental climate with low total annual precipitation compared to other
140 mountain areas at the same elevation. At 1570 m a.s.l., where a weather station is run by the Province
141 of Bolzano, the mean annual air temperature is 6.6 °C and the mean annual precipitation is 569 mm/yr.
142 The latter is estimated to, which increases up to 800-1000 mm/yr at 2000 m a.s.l.. Precipitation
143 typically occurs as snowfall from November to late April, while summer precipitation mainly
144 originates from convective rainfall events. However, snow storms can ~~occur~~ also occur during the
145 summer at the higher elevations. Snow cover is almost complete at least over the upper three quarters
146 of the Saldur catchment (approximately above 2200 m a.s.l.) until late April-early May, when the
147 melting season begins. Typically, at the end of June-early July snow cover amounts to approximately
148 10% of the total catchment area, as revealed by snow surveys and snow cover estimations based on
149 MODIS data (Notarnicola et al., 2013). Permafrost and rock glaciers are most likely present at
150 elevations higher than 2600-2800 m a.s.l., depending on local conditions (Boeckli et al., 2012, see
151 Table 1).

152 The Saldur River has a nivo-glacial regime, with minima recorded during the winter and maxima
153 typically observed in late spring-early summer. The average winter discharge at the catchment outlet
154 during the 2012-2013 winter period was around 0.38 m³/s whereas during summer 2013 was 3.99
155 m³/s. The highest discharge since the start of monitoring (May 2009) was measured during a melt
156 event on 21 June 2013 and reached 25.9 m³/s, whereas the second highest peak was recorded during
157 a rain-~~on-snowfall~~ event on 4 September 2011 and reached 18.2 m³/s. However, these values must be
158 considered approximated due to the uncertainties of the rating curve at high discharge values (see
159 Section 3).
160

161 Geologically, the Saldur basin-catchment belongs to the Matsch Unit, located in the southern Ötztal-
162 Stubai complex and characterized by three main tectonometamorphic events in the Variscan, Permian
163 and Cretaceous periods. The base of the Matsch Unit belongs to the Vinschgau Shear Zone, that
164 changes in the Schlinig fault. The Matsch Unit mainly consists of gneisses, mica gneisses and schists.
165 The land cover within the catchment is dominated by bare rocks and bare soil (47%), grassland (38%)
166 and forest (10%) (based on CORINE90 maps). The main grass vegetation *Nardion strictae* represents
167 mostly the vegetation type at the bottom of the upper valley while the shrub vegetation *Rhododendro-*

Vaccinium covers mostly the valley slope. Haplic Leptosol are present above the tree line (at 2300 m a.s.l.), while forests, especially on the north-facing slopes, are mainly characterized by Haplic Podzols. Managed meadows below 1800 m a.s.l. are mostly characterized by Distric Cambisols. Soil texture can be classified between loamy sand and sandy loam (Bertoldi et al., 2014).

The upper catchment is poorly subjected to weakly affected by human pressures, as only sparse cattle and sheep grazing is present up to 2400 m a.s.l. The uppermost permanently lived building is at 1824 m a.s.l. and a small and steep gravel road goes up to around 2220 m a.s.l. and. Only below 1800 m a.s.l. irrigated and intensively managed meadows are present. A limited net of tracks, mainly hiked during July and August, crosses the middle and the upper part of the catchment. Cattle graze in the area at elevations up to 2400 m a.s.l. but sheep and goats can be found at much higher elevations.

3. Materials and Methods

3.1 Field measurements and sampling

Hydro-meteorological data used in this study were collected in the middle and upper part of the Saldur catchment approximately from April 2011 to October 2013. Precipitation and temperature were measured every 15 minutes by two non-heated weather stations (Onset Corporation, USA), labelled M3 and M4 (Fig. 1) at 2332 and 1998 m a.s.l., respectively, and managed by the Institute for Alpine Environment of EURAC. For data analysis, the average values from these stations were used. Winter precipitation in these stations was validated-estimated using precipitation data and automatic recorded snow height data from a nearby stations of the EURAC network in a wind-sheltered location at the same elevation of the M4 station, by using following the approach suggested by Mair et al. (2013).

Water stage in the main Saldur channel was measured-recorded every ten minutes by-through pressure transducers at the catchment outlet (1632 m a.s.l., station run) by the Hydrographic Office of the Province of Bozen-Bolzano, and at two natural sections, laterally well confined by large immobile boulders, cross sections on the main channel, named Lower Stream Gauge (S3-LSG, 2150 m a.s.l.) and Upper Stream Gauge (S5-USG, 2340 m a.s.l.). The drainage area of these two sub-catchments is 18.6 and 11.2 km², respectively (Table 1). Water stage was converted to discharge by means of Eighty-two (82) salt dilution discharge measurements were taken under different flow conditions, in a range of 0.58 to 4.5 m³/s, repeatedly during the three years. The geometry of the natural cross-sections was monitored over time and different flow rating curves, derived from the salt dilution measurements, were applied through the three years. Water stage was also measured on a tributary on the left side of

202 the valley (T2-SG, 2027 m a.s.l., drainage area of 1.7 km²) but direct discharge measurements were
203 not available to build a reliable flow rating curve. Thus, for tributary T2-SG, stream stage was used
204 throughout the study.

206 Stable isotopes of water and EC were measured in rain water, stream water, groundwater, snow,
207 snowmelt and ice melt. The majority of samples was collected between April and October of each
208 monitoring year but occasional samples were also taken in winter, early spring and late fall, especially
209 at the lowest sampling locations. Bulk precipitation was sampled at five locations at different
210 elevations along a 1000 m gradient (Fig. 1 and Table 2) using a 5-L high-density plastic bottle with
211 a 18.5 cm diameter funnel. A mosquito net was placed inside the funnel to prevent leaves, particles
212 or insects falling into the sampler. Bottles were filled with 1.5 cm of mineral oil to prevent evaporation
213 and isotopic fractionation, and replaced approximately every 45 days in 2011 and roughly monthly
214 in 2012 and 2013. Stream water was manually sampled (grab samples) in the Saldur River at eight
215 locations and in five tributaries between 1775 and 2415 m a.s.l. (Fig. 1 and Table 2). The tributaries
216 were chosen to represent sub-catchments characterized by different hydro-geomorphological
217 properties and size (Table 1).

219 Groundwater was sampled from four springs between 2334 and 2360 m a.s.l. on the right side of the
220 valley (Fig. 1 and Table 2), named SPR1 to SPR4. SPR1 was located at the bottom of a hillslope. The
221 water flow was relatively fast but stopped completely ~~and when~~ the spring dried out in October 2011
222 and 2013. SPR2 was surrounded by rocks in a ponding area and the flow was very slow. SPR3 was
223 located close to the stream and connected to it (water flowing from the spring evidently moved
224 downslope towards the stream). Similarly, SPR4 ~~emerged was characterized by evident bubbling~~
225 from sand sediment and ~~flowing-flowed~~ down to the stream. Samples of stream water and
226 groundwater were collected ~~approximately on a~~ monthly basis.

228 The snowpack was sampled by snow corers. Three snow pits were dug on 8 March 2012 (at 1998,
229 2185, and 2205 m a.s.l.) and two on 6 February 2013 (at 1998 and 2085 m a.s.l.) ~~and snow samples~~
230 ~~were taken at different layers. Two samples were taken from each layer in the snow pits directly with~~
231 ~~the sampling bottles. The samples were stored in portable coolers in the field, and let melting in the~~
232 ~~lab at roughly 20°C. Two samples from the same layers were mixed and analysed. Moreover, three~~
233 samples of fresh snow were collected in the lower part of the catchment after two snowfalls in spring
234 2012. In this case, snow was sampled by means of 1-L plastic bags, stored in a cooler, and let melting
235 at roughly 20°C. A few other snow cores were taken occasionally, in spring and summer, at other

236 locations and higher elevations. Snowmelt was sampled by collecting water dripping from snow
237 patches, residual ~~of the~~ winter snowpack, approximately between 2190 and 2815 m a.s.l.
238 Furthermore, the integrated value of snowmelt during the spring was measured using plastic
239 snowmelt lysimeters (Shanley et al., 2002), with an approximate collecting area of 1 m², connected
240 to a 20-L close bucket by 1-m long plastic tube. A 2 cm layer of mineral oil was put in the bucket
241 during the lysimeter installation to prevent evaporation. Two lysimeters were placed at S3-LSG and
242 one at 2205 m a.s.l. in fall 2011 and two at 2205 and 2225 m a.s.l. in fall ~~2013~~2012. They were
243 emptied in mid-May 2012 and at the beginning of June 2013, respectively. Ice melt was collected by
244 sampling rivulets flowing on the surface of the glacier tongue, approximately at 2800 m a.s.l.
245 Additionally, some samples of water slowly dripping from melting debris-covered ice (part of a
246 disconnected glacier mass) were taken near the glacier snout. Throughout the paper, we refer to
247 glacier melt and debris-covered ice melt to distinguish between the two types of ice melt sampling
248 methods. Snowmelt and ice melt samples were taken occasionally during the summer and early fall
249 of the three monitoring years. Overall, 598 water samples were taken during the observational
250 periods. The position of all field instruments and rainfall, stream water and groundwater sampling
251 locations is displayed in Fig. 1.

252

253 **3.2 Laboratory analysis**

254 All water samples were collected in 50 ml high-density plastic bottles with a double cap, leaving no
255 headspace. The samples were stored in the dark at 4°C before isotopic analysis. The isotopic
256 composition of the water samples was determined at the Laboratory of Isotope and Forest Hydrology
257 of the University of Padova (Italy), Dept. of Land, Environments, Agriculture and Forestry by an off-
258 axis integrated cavity output spectroscopy (model DLT-100 908-0008, Los Gatos Research Inc.,
259 USA). ~~The analys protocol and the procedure adopted to minimize the carry over effect are described;~~
260 ~~see in~~ Penna et al., (2010; 2012). The typical instrumental precision (average standard deviation of
261 2094 samples) is 0.5‰ for δ²H and 0.08‰ for δ¹⁸O. EC was measured in the field using a portable
262 conductivity meter (~~WTW 3410, WTW GmbH, Germany~~) with a precision of ± 0.1 µScm⁻¹.

263

264 **3.3 Data analysis**

265 ~~In order to identify the origin of the air masses that determine precipitation on the study area, and to~~
266 ~~better identify the end-members for runoff Starting from δ²H and δ¹⁸O data,~~ we computed the
267 deuterium-excess (d-excess) for each sample, defined as (Dansgaard, 1964):

268

269 $d - excess = \delta^2H - 8 \delta^{18}O$ ~~+ 10~~ (Eq. 1).

Formatted: Font: Bold

270

271 Low d-excess values indicate that evaporation fractionation has occurred, and this leads to a change
272 in the slope of the relationship between $\delta^{18}\text{O}$ and $\delta^2\text{H}$. The d-excess represents the intercept of the
273 linear fit line between $\delta^{18}\text{O}$ and $\delta^2\text{H}$ data in precipitation at the global scale, named global
274 meteorological water line (GMWL, Craig, 1961) and defined as:

275

276
$$\delta^2\text{H} (\text{‰}) = 8 \delta^{18}\text{O} + 10 \quad (\text{Eq. 2})$$

277

278 The d-excess in precipitation is related to humidity and temperature at the moisture source
279 (Dansgaard, 1964) and therefore is useful to infer the origin of water vapour that determines
280 precipitation in the study area (Cui et al., 2009; Wassenaar et al., 2011; Hughes and Crawford, 2013).
281 In South-Western Europe, precipitation data that show d-excess close to the one of the GMWL
282 typically indicate an Atlantic origin of air masses whereas higher d-excess may reflect the influence
283 of water vapour coming from the Mediterranean basin, for which the local Mediterranean meteoric
284 water line (MMWL) is valid (Gat and Carmi, 1970):

285

286
$$\delta^2\text{H} (\text{‰}) = 8 \delta^{18}\text{O} + 22 \quad (\text{Eq. 3})$$

287

288 The identification of the end-members to surface and subsurface runoff was performed by using d-
289 excess coupled to $\delta^2\text{H}$ data of rainfall, glacier melt and snowmelt, as well as of the streams and
290 springs, and an end-member plot was built.

291 The computation of the snowmelt contribution to groundwater recharge was performed by using a
292 simple two-component separation model (Pearce et al., 1986), based on water and tracer mass
293 balance, as follows:

294

295
$$Q_1 = Q_2 + Q_3 \quad (\text{Eq. 4})$$

296

297
$$Q_1 C_1 = Q_2 C_2 + Q_3 C_3 \quad (\text{Eq. 5})$$

298

299
$$Q_2 = [(C_1 - C_3) / (C_2 - C_3)] \times Q_1 \quad (\text{Eq. 6})$$

300

301 where Q_1 , Q_2 and Q_3 represent three different water components (in this case, spring water, snowmelt
302 and rainfall) and C_1 , C_2 and C_3 represent their tracer concentrations. On the basis of Eq. 6, we

Formatted: Font: Symbol

quantified the percentage of snowmelt contribution to groundwater recharge (SNML %) over the three study years using $\delta^2\text{H}$ data, as follows (Earman et al., 2006; Zhang et al., 2009):

$$SNMLT \% = [(C_{SPR} - C_{RF}) / (C_{SNM} - C_{RF})] \times 100 \quad (\text{Eq. 7})$$

where C_{SPR} is the average isotopic composition of all samples collected from each spring over the three monitoring periods, C_{RF} is the volume-weighted average isotopic composition of the 23 rainfall samples collected at the locations RF4 and RF5 (the ones closest and upstream the selected springs, Table 2 and Fig. 1) and C_{SNM} is the average isotopic composition of 16 snowmelt samples collected from melting snow patches at elevations higher than those of the springs. Similarly, we assessed the seasonal contribution of snowmelt to each spring for each sampling date in 2012 and 2013 (2011 was excluded due to the low number of snowmelt samples available). In this case, C_{SPR} is the isotopic composition of the spring water sample collected on a certain day, C_{RF} is the volume-weighted average isotopic composition of the rainfall samples collected at the locations RF4 and RF5 during the period previous to the sampling day, and C_{SNM} is the (average) isotopic composition of the snowmelt sample(s) collected on that day. The 70% uncertainty in the separation of the two components was estimated through the method suggested by Genereux (1998) that takes into account the difference between the isotopic composition of the components and the variability (expressed by the standard deviation) of the isotopic composition of each component. The smaller the difference and the larger the variability, the higher the uncertainty.

Given the covariance between $\delta^2\text{H}$ and $\delta^{18}\text{O}$ values of all samples, we reported in the paper only $\delta^2\text{H}$ values in cases the plots and analyses throughout the paper where information coming deriving from both isotopes were redundant, we reported only results referring to $\delta^2\text{H}$ values.

4. Results and Discussion

4.1 Tracer concentration in different waters

The different waters sampled in the Saldur catchment during this study showed a marked variability in tracer concentration (Fig. 2). Over the entire dataset, $\delta^2\text{H}$ values ranged from -26.1‰ to -202.0‰ and EC ranged from 1 μScm^{-1} to 461 μScm^{-1} . Rainfall and winter snowpack samples were characterized by the most positive and the most negative isotopic composition, respectively, with median values of -65.0‰ and -158.9‰ in $\delta^2\text{H}$, respectively. Overall, snowmelt was intermediate had values between rainfall and snowpack (median $\delta^2\text{H}$ = -122.9‰) whereas ice melt was more enriched in heavy isotopes (median $\delta^2\text{H}$ = -101.3‰). Stream water from the main stream and the tributaries, and groundwater from the springs had similar isotopic composition (median $\delta^2\text{H}$ = -105.2‰, -103.4‰

Formatted: Font: Symbol

and -104.7‰, respectively) but still statistically different isotopic compositions (Kruskal-Wallis test significant at 0.05 level).

The median EC of rainfall (Fig. 2, panel b) was $8 \mu\text{Sem}^{-1}$, thus lower than the EC typically measured in precipitation both in urban catchments (e.g., Pellerin et al., 2008; Meriano et al., 2011) and in other mountain catchments in more natural settings (e.g., Lambs, 2000; Zabaleta and Antigüedad, 2013). Low EC in rainfall indicates low concentration of solutes and suggests a little or negligible influence of air masses coming from the Mediterranean Sea basin, rich in salts and therefore characterized by higher EC (see also Section 4.2). The median EC of snowmelt (from patches of old snow and from the snowmelt ~~samplers-lysimeters~~ as a whole) and ice melt (glacier melt and debris-covered ice melt as a whole) was also low and very low, of $12 \mu\text{Sem}^{-1}$ and $2 \mu\text{Sem}^{-1}$, respectively. Thus, the isotopes isotopic composition allowed to characterize the ice melt signature, compared to that of rainfall, and snowmelt and ice melt allowed, for a more uniquely clearer separation of these end-members than EC. The median EC of stream water in the tributaries and groundwater was similar (232 and $222 \mu\text{Sem}^{-1}$; respectively) and higher than that of the Saldur River ($160 \mu\text{Sem}^{-1}$) that which clearly reflected the contribution of low EC snowmelt and ice melt to streamflow (Section 4.7). EC samples of stream water and groundwater showed statistical differences even more marked than those shown by $\delta^2\text{H}$ data (Kruskal-Wallis test significant at 0.01 level). This reflects the fact that all expected water sources contributing to streamflow during rainfall events and melting periods (rainfall, snowmelt and ice melt) had low values of EC but contrasting isotopic composition that compensated when mixed in the Saldur River.

4.2 Isotopic composition of rainfall

The linear relationship between $\delta^{18}\text{O}$ and $\delta^2\text{H}$ composition of rainfall data collected at different elevations in the Saldur catchment defined a local meteorological water line (LMWL), expressed as (Fig. 3):

$$\delta^2\text{H} (\text{‰}) = 8.1 \delta^{18}\text{O} + 10.3 \quad R^2 = 0.99, n = 66 \quad (\text{Eq. 8})$$

This relationship is slightly different from the LMWL of Northern Italy (Longinelli and Selmo, 2003; Longinelli and Stenni, 2008, Table 3) defined as:

$$\delta^2\text{H} (\text{‰}) = 7.7 \delta^{18}\text{O} + 9.4 \quad (\text{Eq. 9})$$

and also from the LWML found by Chiogna et al. (2014) for a station at 1176 m a.s.l. in a glacierized Alpine catchment between the Ortles-Cevedale and the Adamello-Presanella massifs (Northern Italy, approximately 44 km South in a straight line from the Saldur catchment, [Table 3](#)), ~~defined as:~~

$$\delta^2H (\text{‰}) = 7.6 \delta^{18}O + 2.7 \quad (\text{Eq. 10}).$$

Conversely, the LMWL in the Saldur catchment is quite similar to the one derived at the highest elevation ([2731 m a.s.l.](#)) reported by Chiogna et al. (2014) in similar climatic conditions ([Table 3](#)), ~~defined as:~~

$$\delta^2H (\text{‰}) = 8.0 \delta^{18}O + 7.8 \quad (\text{Eq. 11}).$$

It is evident that the slope of the Saldur LMWL (10.1) is higher than that of the other Northern Italian sites at lower elevations (7.7 and 7.6, [Eqs. 9 and 10, respectively Table 3](#)), but approximately the same to that in a mountain region at higher elevation (8.0, [Eq. 11 Table 3](#)). More interestingly, both the slope and the d-excess of the Saldur LMWL are nearly identical to those of the GMWL (Eq. 2) and d-excess is noticeably different from that of the MMWL (Eq. 3). Although a full comparison among these relationships cannot be made because the LMWL at our site did not include samples collected during the winter, this reveals that precipitation (at least during late spring, summer and early fall [of the three observation years](#)) in the Saldur area, and likely in other left-side lateral valleys of the Upper Vinschgau valley, was predominantly originated by air masses developing on the Atlantic Ocean, with limited influence by inflow of water vapour from the Mediterranean sea. This confirms what [was](#) indicated by the very low EC observed in rainfall (Section 4.1). [Moreover, these observations are in agreement with the fact that the complex topography of South Tyrol leads to the coexistence of many different microclimates and precipitation patterns \(Brugnara et al., 2012\).](#)

Figure 3 also highlights the clear and expected temperature-dependent seasonality (e.g., Wassenaar et al., 2011) with heavier isotopic values occurring during the summer, lighter values occurring during the fall and intermediate values generally occurring during the spring, and partially overlapping with the most negative summer samples and the most positive fall samples. In addition, ~~the inset reported in Fig. 3 displays the variation of average δ^2H of rainfall samples (n=8) as a function of the station elevation, revealing a~~ [we observed a](#) marked altitude effect (Araguás-Araguás et al., 2000; [inset of Fig. 3](#)), recognized in almost all mountain ranges worldwide (Poage and Chamberlain, 2001). Particularly, the linear relationship between the average isotopic composition of rainfall samples and

elevation in the Saldur catchment yielded an isotopic depletion rate of -1.6‰ for $\delta^2\text{H}$ and -0.23‰ for $\delta^{18}\text{O}$ per 100 m rise in elevation. This gradient is steeper than that found in a snowmelt- and glacier melt-dominated Andean catchment, Chile (Ohlanders et al., 2013), and by Chiogna et al. (2014), and is gentler than that in the Kumaon Himalayas, India (Kumar et al., 2010). However, the gradient is fully consistent with that in Kashmir Himalaya (Jeelani et al., 2013) and with the one reported by Longinelli et al. (2006) for an Alpine region in North-Western Italy.

Elevation played also a role on the spatial variability of d-excess in precipitation. Although the relationship was less strong than the one between elevation and $\delta^2\text{H}$ and $\delta^{18}\text{O}$ in rainfall, our data (not reported) showed that d-excess (the average of data available for all five sampling locations, n=8) increased roughly linearly ~~of by~~ 0.2‰ per 100 m rise in elevation ($R^2=0.69$, n=5, significant at 0.1 level). This effect was also reported for other mountain areas (Cui et al., 2009; Kumar et al., 2010; Jeelani et al., 2013). In some cases, the increase of d-excess with altitude was reported to be mainly present at high relative humidity (Gonfiantini et al., 2001; Windhorst et al., 2013) which is not the case of the study area. In the Saldur catchment, this effect may be attributed to higher relative humidity at higher elevations due to snow and ice melting which tends to enhance the kinetic fractionation process during evaporation (cf. Peng et al., 2004). ~~However, additional unknown factors (Gat et al., 2000) might be claimed to explain the observed altitude effect of d-excess.~~

4.3 Isotopic composition of snow, snowmelt and ice melt

Snow samples taken from the winter snowpack covered a broad isotopic range, ~~spanning from -134.9‰ to -202.0‰ in $\delta^2\text{H}$ and from -18.34‰ to -26.46‰ in $\delta^{18}\text{O}$~~ (Fig. 4), reflecting a wide variability in air temperature that may have occurred also during the winter. Moreover, snow samples ~~plotted~~ fell well on the LMWL (and therefore on the GMWL), as also confirmed by the slope and interception values very similar to those of the LMWL (Table 34). This ~~was also found for a set of snow-dominated catchments in Switzerland (Dietermann and Weiler, 2013) and~~ indicates a similar geographical origin of precipitation during the winter with respect to the other seasons. ~~However, we must mention that the range in the isotopic composition of snow samples was likely underestimated, due to the uncertainty associated with finding sampling locations representative for the isotopic signature of snowpack over the entire catchment. Indeed, in addition to altitude and seasonal effects, several other factors such as micro- and macro-topography, relocation of snow through wind drift and avalanches, and enrichment of heavy isotopes in upper layers of the snowpack depending on the sun exposure can contribute to significantly enhance the spatial and temporal variability of the isotopic composition of snowpack (Dietermann and Weiler, 2013).~~ Samples collected from melting snow

439 patches showed a wide isotopic range too, ~~varying from -106.1‰ to -165.4‰ in $\delta^2\text{H}$ and from~~
440 ~~-14.26‰ to -21.47‰ in $\delta^{18}\text{O}$~~ (Fig. 4). This likely reflects the different elevations ~~where-at which~~ the
441 samples were collected and, at the same time, the progressive seasonal isotopic enrichment that
442 snowpack underwent during the melting process (Taylor et al., 2001; Lee et al., 2010). Meltwater
443 samples of snow patches ~~laid-fell~~ on the LMWL too (Fig. 4), and were characterized by values of
444 slope and intercept very similar to those of the LMWL (Table 34), indicating no or negligible
445 secondary fractionation effects due to evaporation during deposition and melting processes.
446 Alternatively, this might also suggest a high consistency of isotopic fractionation as well as a temporal
447 covariation of meltwater isotopic values at the catchment scale (Zhou et al., 2014). Winter- and
448 spring-integrated snowmelt samples taken from the lysimeters also followed the LMWL but were
449 slightly below ~~it-the line~~ (Fig. 4) and showed a slightly smaller slope and intercept (Table 34).
450 Moreover, except for three samples, snowmelt samples collected from lysimeters were isotopically
451 heavier than snowmelt samples collected from snow patches. This difference was related to some
452 possible contamination from ~~relatively less negative~~ precipitation during the spring, relatively
453 enriched in heavy isotopes. The three samples with more negative values were collected in spring
454 2012 from snow lysimeters ~~localized-located~~ close to the stream at S3-LSG, in a zone where the
455 valley is relatively narrow and direct sunlight is limited.

456
457 Ice melt samples generally plotted on the LMWL but, in accordance to Gooseff et al. (2006), the
458 slopes and the intercepts of their $\delta^{18}\text{O}$ - $\delta^2\text{H}$ relationships for both glacier melt and debris-covered ice
459 melt were slightly smaller than those of the LMWL (Table 34). A comparison of the isotopic
460 composition of glacier meltwater in the Saldur catchment with samples taken in other parts of the
461 globe reveals the variability of dominant climatic conditions. Saldur glacier melt was more depleted
462 compared to the Mafengu River, China (Yang et al., 2012), similar to the Ganga River catchment in
463 the Himalayan foothills (Maurya et al., 2011) and in the Langtang and Dudh Kosi basins in Nepal
464 Himalaya (Racoviteanu et al., 2013). However, it was heavier than that in the Wind River Range in
465 the American Rockies (Cable et al., 2010) and a Central Andean catchment (Ohlanders et al., 2013)
466 and, not surprisingly, much heavier than that found at the Imersuaq Glacier, West Greenland (Yde
467 and Knudsen, 2004).

468
469 The isotopic range of glacier melt and debris-covered ice melt samples collected in the Saldur
470 catchment was similar (Fig. 4), ~~with average $\delta^2\text{H}$ =-102.3‰ and standard deviation=7.8‰ for glacier~~
471 ~~melt (n=16), and average $\delta^2\text{H}$ =-100.2‰ and standard deviation=4.9‰ for debris-covered ice melt~~
472 ~~(n=9)~~. However, glacier melt typically showed higher d-excess ~~(12.7‰ vs. 11.0‰)~~ but similar

variability of d-excess (~~standard deviation of 1.2‰ vs. 1.4‰~~) compared to debris-covered ice melt. This difference was likely associated to the aforementioned increase in d-excess with elevation (Section 4.2), since the rivulets sampled on the glacier surface originated at higher elevations compared to the debris-covered ice collected nearby the glacier snout. Moreover, the expected lower melt rate due to the debris coverage, compared to the melt occurring on the bare glacier surface, might have also determined secondary evaporation effects (confirmed by the slightly smaller slope compared to glacier melt, Table 34) contributing to the difference in d-excess between the two subsets. However, the most striking difference between the two types of ice melt samples lays in the much higher and more variable EC of meltwater derived from ice bodies covered by debris (~~average=66 μSem^{-1} , standard deviation=40 μSem^{-1} ; n=6~~) compared to the extremely low (almost distilled) and little variable EC of glacier meltwater (~~average=2 μSem^{-1} , standard deviation=0.7 μSem^{-1} ; n=16~~). This difference, reflecting the very high variability in EC of all ice melt samples (glacier melt and debris-covered ice melt, Fig. 2, panel b), was not unexpected considering the contact that the latter had with rocks and fine debris that could release salts thereby increasing the EC of meltwater.

4.4 Isotopic composition of stream water and groundwater

The isotopic composition of stream water showed a narrower range compared to rainfall, snowmelt and ice melt (Fig. 2, panel a) indicating that waters originating from upstream sources mixed to give composite stream water (Dalai et al., 2002; Maurya et al., 2011). The slope of 7.9 of the $\delta^{18}\text{O}$ - $\delta^2\text{H}$ relationship of stream water in the Saldur River (~~Table 4~~) was similar to that of rainfall (Fig. 3) and especially to that of snowmelt (Table 34), indicating that these water sources underwent similar fractionation processes reflecting well the isotopic signal of this water source. On the contrary, groundwater and stream water in the tributaries showed lower slopes of the $\delta^{18}\text{O}$ - $\delta^2\text{H}$ relationship compared to the Saldur River waters and to rainfall samples (and therefore a departure from the LMWL, not shown) suggesting post-precipitation evaporation during the groundwater recharge process (Maurya et al., 2011), as discussed in section 4.98.

4.5 Identification of end-members

The average values of $\delta^2\text{H}$ plotted versus d-excess for all stream water and groundwater samples fell within a triangular domain defined by the average $\delta^2\text{H}$ and d-excess (Machavaram et al., 2006) of rainfall, snowmelt and glacier melt (Fig. 5). Unfortunately, since we were able to measure rainfall intensity but not snowmelt and glacier melt intensity, only the $\delta^2\text{H}$ and d-excess values of rainwater samples were volume-weighted whereas snowmelt and glacier melt were not. This could affect mass

balance computations but it is reasonable to assume that this would not change the general evidence provided by Fig. 5. Indeed, despite the large variability of measurements in all waters (evidenced by the long horizontal and vertical error bars), the mixing plot clearly reveals the importance of snowmelt and glacier melt as end-members in the study catchment, playing therefore a major role on the runoff regimes of the Saldur River and of its tributaries, as also observed in other glacierized catchments (Zhang et al., 2009; Dahlke et al., 2013; Olhanders et al., 2013). However, it must be mentioned that we normally collected samples during no-rain periods, and therefore the contribution of rain water to the isotopic and EC composition of stream water and groundwater was likely underestimated. Although the error bars of samples within the triangular space largely overlapped, it is interesting to note that samples taken in the main stream were closer to the glacier melt end-member than the samples collected in the tributaries, and that the samples collected from the springs fell closer to the snowmelt end-member than stream water samples. This indicates, as expected, that glacier melt was a more important contributor to runoff in the main stream, distinctly glacier fed, compared to the tributaries, and suggests an important role of snowmelt on groundwater recharge (Section 4.89). Snowpack samples were not included in the mixing plot simply because winter snowpack cannot be considered as a direct hydrological input.

523

524 4.6 Temporal hydrological dynamics

525 The three observational periods considered in this study showed different hydro-meteorological characteristics (Fig. 6). The average temperature over the April 1-October 31 period was similar for 526 the three years (6.7, 6.5 and 6.3°C for 2011, 2012 and 2013, respectively) but the temporal variability 527 slightly differed. Most of all, cumulative precipitation was noticeably different, with 536, 467 and 528 only 380 mm over the same period in 2011, 2012 and 2013, respectively. However, although 2013 529 was the driest year, streamflow and water stage at the gauging stations, especially at S5-USG, showed 530 marked responses, suggesting important contributions of meltwater. At the end of April-beginning of 531 May, when the melting season started, streamflow in the main stream (Fig. 6, panels g-l) and water 532 stage in the tributary T2-SG (Fig. 6, panels m-o) were typically low with values close to the winter 533 baseflow (below $0.5 \text{ m}^3/\text{s}^+$ at S5-USG, $1 \text{ m}^3/\text{s}^+$ at S3-LSG and 5 cm at T2-SG). Then, streamflow 534 noticeably increased during the warmer months (June-August) up to $3\text{-}4 \text{ m}^3/\text{s}^+$ at S5-USG, $6\text{-}7 \text{ m}^3/\text{s}^+$ 535 at S3-LSG and 25-30 cm at T2-SG, and started to recede in September, reflecting the combination 536 of limited snow cover and incoming radiation too small to produce important melt. Additionally, 537 streamflow showed a marked diurnal variability (Josth et al., 2012; Uhlmann et al., 2013), particularly 538 in the main stream and slightly less evident in the tributary, with clear fluctuations dependent on daily 539

Formatted: Not Superscript/ Subscript

Formatted: Not Superscript/ Subscript

Formatted: Not Superscript/ Subscript

Formatted: Not Superscript/ Subscript

540 temperature oscillations that triggered the release of meltwater to the stream network (Fig. 6, panels
541 d-o).

542

543 At the seasonal scale, the melting dynamics seemed to override the role of rainfall on streamflow
544 variability. Typical rainfall events were characterized by daily cumulative amounts of less than 10
545 mm that produced small streamflow response and limited sediment transport (Mao et al., 2014).
546 However, the highest streamflow peaks were associated ~~to-with~~ relatively intense rainfall events. For
547 example, 19.6 mm of rain fell in four hours on September 4, 2011 and produced hourly streamflow
548 hourly peaks of $5.3 \text{ m}^3/\text{s}^+$ at S5-USG, $8.0 \text{ m}^3/\text{s}^+$ at S3-LSG and a water stage peak of 37 cm at T2-
549 SG, observed almost simultaneously at all three gauging locations.

550

551 4.7 Spatio-temporal dynamics of tracer concentration in stream water and groundwater

552 4.7.1 Temporal variability of stream water and groundwater EC and $\delta^2\text{H}$

553 The isotopic composition of stream water (Fig. 6, panels g-o) did not reflect the seasonal variation of
554 isotopes in rainfall isotopic composition, with the less negative values occurring during the warmest
555 periods (Section 4.2) but tended to mirror it (Jeelani et al., 2013). Indeed, the samples collected in the
556 Saldur River and its selected tributaries revealed that during the late spring and the beginning of the
557 summer (June-July) $\delta^2\text{H}$ in stream water was relatively depleted in heavy isotopes (ranging
558 approximately between -115 and -110‰), then increased during mid-late summer ~~up~~ to values close
559 to the baseflow background isotopic composition (Fig. 6). Similarly, EC was relatively high before
560 the beginning of the melting period (up to approximately $250 \text{ }\mu\text{S}/\text{cm}^+$ at S3-LSG), then decreased
561 below $100 \text{ }\mu\text{S}/\text{cm}^+$ during the melting season and increased to background values in mid-late October
562 (Fig. 6). ~~This pattern was less clear in 2011 in the main stream (Fig. 6, panels g and j) because samples~~
563 ~~were collected at different times of the day and therefore the variability in tracer composition, due to~~
564 ~~the daily streamflow fluctuations induced by meltwater inflows, masked the seasonal evolution.~~
565 However, ~~g~~Given the very low EC and the significantly more negative values of snowmelt and ice
566 melt compared to rainfall (Fig. 2), the general pattern suggests a remarkable ~~(even though not easily~~
567 ~~quantifiable)~~ contribution of meltwater to runoff in the Saldur catchment, confirming the results of
568 the end-member mixing analysis (see Fig. 5 and Section 4.7.3).

569

570 This trend was also revealed by the $\delta^2\text{H}$ and EC of four locations along the Saldur River, ~~for which~~
571 ~~we collected samples approximately monthly during all three monitoring years, of three tributaries~~
572 ~~for which we have the most numerous data~~ and of the four selected springs (Fig. 7). We show here
573 data from the Saldur locations where we collected samples approximately monthly during all three

Formatted: Not Superscript/ Subscript

Formatted: Not Superscript/ Subscript

574 monitoring years, and from the three tributaries for which we have the most numerous measurements.
575 There was an overall pattern of more negative isotopes and relatively low EC at the beginning and at
576 the peak of the melting season ~~was evident~~. Analogously, less negative isotopes and higher EC were
577 observed at the end of the season. Overall, this pattern was temporally consistent for stream water,
578 both in the main stream and in the tributaries, and for groundwater. The increasing trend in isotopic
579 composition and EC of the springs and the tributaries (generally with a negligible glacierized area
580 compared to that of the main stream sub-catchments, see Table 1) likely reflects the decreasing
581 contribution of snowmelt over the season. ~~Moreover, the relatively fast dynamics of tracer~~
582 ~~concentrations in the springs suggested low residence times in the catchment (Jeelani et al., 2010).~~
583 Isotopes in the Saldur River in August 2013 (Fig. 7, panel a) were noticeably less negative compared
584 to the previous sampling time and disagreed with patterns showed by the isotopic composition of the
585 springs (Fig. 7, panel c) ~~that continued the negative trend before increasing on the last sampling date.~~
586 One reason for this difference could be related to the lagged arrival of the snowmelt contribution to
587 the springs but this should be verified by means of additional data and possibly modelling application.
588

589 4.7.2 Spatial variability of stream water and groundwater EC and δH

590 The consistency of temporal patterns ~~over space, among~~across the different locations, was
591 particularly remarkable for the Saldur River locations and for springs SPR1-3 (Fig. 7, panels a and c,
592 respectively). Overall, location S8, higher in elevation and closer to the glacier snout (Table 2),
593 showed the most extreme δ^2H and the lowest EC likely because it was more directly influenced by
594 meltwater inputs. S3-LSG and S1, the locations more downstream, showed the highest EC, due to the
595 comparatively higher contribution of groundwater. However, S3-LSG was characterised by relatively
596 more negative δ^2H compared to S1 due to the inflow of the highly isotopically depleted tributary at
597 location T4 (data not shown). SPR4 showed a clearly different isotopic composition and EC
598 concentration and different patterns compared to the other three springs. So far, we do not have
599 experimental data to explain these differences but a more detailed analysis of groundwater
600 geochemical and microbiological composition at different locations in the Saldur catchment is in
601 progress.
602

603 4.7.3 Seasonal change in snowmelt and ice melt contribution to runoff

604 ~~Data of stream water tracer concentration collected in 2011, 2012 and 2013 at the same time of the~~
605 ~~day at four selected locations along the Saldur River (S1, S3-LSG, S5 and S8) were grouped according~~
606 ~~to the month of sampling and displayed as box-plots (Fig. 8).~~ Figure 8 shows a box-plot of the stream
607 water isotopic composition of four selected sampling locations along the Saldur River (S1, S3-LSG,

Formatted: Font: (Default) Times New Roman, 12 pt

Formatted: Font: (Default) Times New Roman, 12 pt

S5 and S8) for the months June to October. Stream water was relatively depleted in heavy isotopes in June, isotopically heavier and characterized by a large variability in July and slowly increasingly enriched in heavy isotopes in August, September and October (Fig. 8, panel a). Interestingly, EC showed a different pattern, with low values and similar variability in June, July (slightly lower) and August and markedly higher distributions in September and October (Fig. 8, panel a). Although this plot masks the inter-annual variability of tracer concentration and the number of samples is limited, the observation of the different dynamics of the two tracers gives some hints on the seasonal switch of the most important contributors to runoff of the Saldur River. Indeed, the negative $\delta^2\text{H}$ and low EC values found in June might reflect a major contribution of snowmelt, depleted in heavy isotopes and with low EC (Fig. 2). The even lower EC but less negative and more variable isotopes in July might reflect a mixed contribution of snowmelt and glacier melt that had extremely low EC but less negative isotopic composition (Fig. 2). The still low EC but the relatively heavier isotopes in August likely might reflect a major contribution of glacier melt. Finally, the more enriched $\delta^2\text{H}$ and the higher EC in September and October suggest a little or negligible diminishing contribution of meltwater to the Saldur River, especially in October when the variability in the isotopic composition of stream water was very small.

Formatted: Font: (Default) Times New Roman, 12 pt

The same conclusions can be drawn when looking at the spatio-temporal variability of tracer concentration at the same four selected locations along the main stream for different sampling days in 2013, i.e., the year where-for which we have more data collected at approximately the same time of the day on different dates (Fig. 9). The low EC and the relatively heavier isotopes in stream water in August reflected particularly well the tracer composition of glacier melt (average $\delta^2\text{H}=102.3\text{‰}$, standard deviation=7.8‰; average EC=2.1 μScm^{-1} , standard deviation=0.7 μScm^{-1}) suggesting its dominant contribution to streamflow later in the melting season, when most of the catchment is typically snow-free. Moreover, the spatial pattern of tracer concentration along the stream was consistent among the different dates for EC (except for the decreasing value at S1 in October, Fig. 9, panel b) and more gentle but still fairly similar for $\delta^2\text{H}$. This general temporal persistence of spatial patterns of tracer concentration indicates that the contribution of different water sources and of tributaries to the stream was continuous over time, i.e., all water sources and all tributaries, although carrying a possibly different isotopic and EC signature, gave continuous contributions over time, also revealing a good water mixing in the stream.

Formatted: Not Superscript/ Subscript

4.8 Role of snowmelt on groundwater recharge

The application of the isotope-based two component separation model to spring water data (Eq. 7) allowed us to quantify the relative contribution of snowmelt to groundwater recharge, qualitatively assessed by the visual inspection of the temporal variability of tracer concentration in the selected springs (Section 4.7). Despite some inter-annual variability, snowmelt contributions to spring recharge were relatively low in June (Fig. 10), when the stream showed a snowmelt tracer signature (Fig. 8), and highest in July and August (Fig. 10), when most of the catchment area was snow-free. This indicates a relative longer time for the snowmelt signal to appear in groundwater than in stream water, suggesting complex subsurface flow paths and long recharge times. The seasonal pattern was similar for the four springs, revealing a spatial consistency in the seasonal trend of groundwater recharge, at least at the small spatial scale of the four springs we investigated (Fig. 10). Our results also revealed that, overall over the three study years, snowmelt played a relevant role on groundwater composition in the Saldur stream compared to rainfall, with overall contributions ranging from 58% ($\pm 24.5\%$) for SPR4 to 72% ($\pm 19.5\%$) for SPR2 (Table 5). In this case, the average snowmelt used as an input for the separation model included all measurements taken over the three years in different months, and therefore showing a broad range of isotopic values. As a consequence, the standard deviation was large. This explains the general higher uncertainties in the estimates of the overall snowmelt contribution to groundwater (Table 5) compared to the estimates of snowmelt contribution to groundwater calculated for different sampling times over the season (small vertical error bars in Fig. 10), for which the snowmelt input values of each sampling day derived from one individual sample or from the average of few samples isotopically similar, and therefore characterized by small standard deviations. Including ice melt data (both glacier and debris-covered ice melt) in the model gave inconsistent results, likely indicating the negligible contribution of ice melt to groundwater recharge. The very similar fractions among SPR1-3 and the different fractions compared to SPR4 agree, as expected, with the observed differences in the isotopic composition of the four springs (Fig. 7, panel c and f). The comparatively minor role of summer precipitation in recharging groundwater is also confirmed by considering that the average isotopic composition of the springs was not consistent with the much more positive average isotopic composition of rainfall (Fig. 2, panel a). When spring $\delta^2\text{H}$ was plotted on a rainfall $\delta^2\text{H}$ vs. elevation plot (not shown) to estimate the elevation of groundwater recharge (e.g., Jeelani et al., 2010) we obtained inconsistent results, i.e., the ~~elevation of recharge~~ elevation was found to be much higher than the highest peak in the study area. This demonstrates the noticeably greater contribution of snow precipitation compared to liquid precipitation. This is probably not surprisingly considering the low precipitation amounts that characterize the study area during the summer. However, these results are important for the development of a perceptual model of the hydrological functioning of the Saldur catchment.

Moreover, these results are in agreement with the upper limit of the isotopic-based estimates of the role of snowmelt on groundwater recharge in the South-Western United States (Earman et al., 2006) and confirm previous observations from other high-elevation catchments (Earman et al., 2006; Jeelani et al., 2010; 2013).

679

680 5. Limitations of the research and concluding remarks

Spatially-distributed samples of rainfall, snowmelt, ice melt, groundwater and stream water were collected over three years in the glacierized Saldur catchment in the Eastern Italian Alps and analysed for stable isotopes of water and EC, allowing us to identify the main end-members and to explore the spatio-temporal variability of water sources. Data collection in such a high-elevation and complex terrain proved to be particularly challenging, and some issues arose. For instance, sampling at higher temporal frequency might have allowed us to explore some short-time responses in tracer concentration and detect some finer dynamics (e.g., Neal et al., 2013). Moreover, samplings were not always taken at the same time of the day ~~among-over~~ the three years, preventing us to make comparisons on a more extended subset of data. More importantly, we were not able to sample permafrost ~~(for instance, from rock glaciers)~~ and winter precipitation beside snowpack (we experienced snowfall collectors failures for two consecutive winters), likely yielding an incomplete overview of all potential end-members in the study catchment. Analogously, as mentioned above, the lack of sampling during rain periods probably provided an underestimation of the role played by rain water on the isotopic and EC composition of stream water.

695

Despite these limitations, our study corroborated preliminary observations (Penna et al., 2013) and provided new insights on-into the isotopic characterization of waters in high-elevation Alpine basins, allowing us to take advantage of the enhanced tracer capability derived from the combined use of EC and water stable isotopes for identifying end-members. Particularly, our results shed new light on the main sources of water contributing to runoff and their spatio-temporal variability, information that were still missing in glacierized areas of South-Tyrol and are still very limited for the entire Southern Alps. ~~Particularly, from~~ a methodological point of view, this research provided one of the largest isotopic database in glacierized catchments that we are aware of, even larger than some very robust datasets recently published (e.g., Ohlanders et al., 2013; Chiogna et al, 2014). Furthermore, our study was the first one, as far as we know, to provide samples of EC and isotopic composition of actual glacier melt in the Italian Alps, i.e., meltwater flowing directly on the glacier surface and not water discharging from the glacier snout (possibly mixed with groundwater inflows). This allowed a better characterization of the tracer concentration of this end-member. Finally, the observation periods that

spanned three years across various seasons allowed us to identify temporally-invariant behaviours in tracer concentrations as well as to compare the inter-annual variability of water source dynamics, providing a broader idea of hydrological behaviours under different conditions.

In conclusions, the main results are the following:

- ~~A marked variability in EC and isotopic composition of all sampled waters was evident, indicating a highly complex signature of water within the catchment. The combined signature provided by the two tracers yielded a clear distinction between input sources to the system, allowing us to identify snowmelt and glacier melt as the main end-members for stream water and groundwater, with a secondary role played by rainfall;~~
- Rainfall samples delineated a LMWL remarkably similar to the GMWL, suggesting a predominantly oceanic origin of air masses in the study area. In addition to the seasonal effect, a clear altitude effect was observed for rainfall samples, with an isotopic depletion rate of -1.6‰ for $\delta^2\text{H}$ and -0.23‰ for $\delta^{18}\text{O}$ per 100 m rise in elevation;
- A marked variability in EC and isotopic composition of all sampled waters was evident, indicating a highly complex signature of water within the catchment. The combined signature provided by the two tracers yielded a clear distinction between input sources to the system, allowing us to identify snowmelt and glacier melt as the main end-members for stream water and groundwater, with a secondary role played by rainfall;
- ~~Snow, snowmelt and ice melt samples fell along the LMWL, indicating little or negligible evaporation during the post-deposition processes. On the contrary, the isotopic composition of groundwater samples showed a post-precipitation evaporation effect.~~
- The temporal dynamics of tracer concentrations and, particularly, the different dynamics of EC with respect to $\delta^2\text{H}$ revealed a change in the main water source to the Saldur River runoff over the season, with snowmelt being the major contributor to streamflow during the first and central part of the melting period (June, July), whereas later in the summer, when most of the snow disappeared from the catchment, glacier melt contributed significantly. Despite such dynamics are well known in high-elevation catchments, their clear detection based on tracers is ~~quite~~ remarkable from a methodological perspective;

- The contribution of snowmelt to groundwater recharge, quantified by using an isotope-based two component separation model, generally decreased during the season, varying between 93% ($\pm 1\%$) in August and 21% ($\pm 3\%$) in September. The overall contribution of snowmelt to groundwater recharge, quantified by using an isotope-based two component separation model, over the three years ranged between 58% ($\pm 24\%$) and 72% ($\pm 19\%$), revealing the marked importance of snowmelt for subsurface water storage in the Saldur catchment.

~~Overall, these results shed new light on the main sources of water contributing to runoff and their spatio-temporal variability, information that were still missing in glacierized areas of South Tyrol and are still very limited for the entire Southern Alps. These data provide preliminary and qualitative information on the temporal evolution of meltwater to the Saldur River network that will be compared with satellite images and modelling results. Moreover, in an ongoing work, two- and three-component hydrograph separation models, based on hourly tracer data, are being applied to selected runoff events in the study years (preliminary results in Penna et al., 2013). These analyses will permit quantitative estimates of the contribution of ice melt and snowmelt to stream water in different periods of the seasons and will lead to a better understanding of the role of meltwater dynamics on streamflow generation in high elevation glacierized catchments of the Alps.~~

Acknowledgements

This work was financially supported by the research projects “Effects of climate change on high-altitude ecosystems: monitoring the Upper Match Valley” (Free University of Bozen-Bolzano) and “EMERGE: Retreating glaciers and emerging ecosystems in the Southern Alps” (Dr. Erich-Ritter- und Dr. Herzog-Sellenberg-Stiftung im Stifterverband für die Deutsche Wissenschaft). Technical Support was ~~also~~ provided by the Dept. of Hydraulic Engineering and Hydrographic Office of the Autonomous Province of Bozen-Bolzano. The project “HydroAlp”, financed by Autonomous Province of Bozen-Bolzano, ~~and~~ partly supported the work of G. Bertoldi. G. Niedrist of EURAC is thanked for his work in maintaining the meteorological stations. Giulia Zuecco (University of Padova) is warmly thanked for the laser spectroscopy isotopic analysis. We thank Enrico Buzzi and Raffaele Foffa for support in field work. The first author is grateful to ~~Hja-H. J.~~ van Meerveld (~~VU~~ University of ~~Amsterdam~~Zurich) for discussions during a field trip, and to James W. Kirchner (ETH, Zurich) for discussions on the preliminary results. Two anonymous reviewers are thanked for their constructive comments.

References

777 Araguás-Araguás, L., Froehlich, K., Rozanski, K., 2000. Deuterium and oxygen-18 isotope
 778 composition of precipitation and atmospheric moisture. *Hydrol. Process.*, 14:1341–1355. doi:
 779 10.1002/1099-1085(20000615)14:8<1341::AID-HYP983>3.0.CO;2-Z
 780

781 Bertoldi G., Della Chiesa S., Notarnicola C., Pasolli L., Niedrist G., Tappeiner U., 2014. Estimation
 782 of soil moisture patterns in mountain grasslands by means of SAR RADARSAT 2 images and
 783 hydrological modelling. *J. Hydrol.* (in review)

784

785 [Brugnara, Y., Brunetti, M., Maugeri, M., Nanni, T., Simolo, C., 2012. High-resolution analysis of](#)
 786 [daily precipitation trends in the central Alps over the last century. *International Journal of*](#)
 787 [Climatology 32, 1406–1422. doi:10.1002/joc.2363](#)
 788

789 Boeckli, L., Brenning, A., Gruber, S., Noetzi, J., 2012. A statistical approach to modelling permafrost
 790 distribution in the European Alps or similar mountain ranges. *Cryosph.* 6(1), 125–140.
 791 doi:10.5194/tc-6-125-2012
 792

793 Cable, J., Ogle, K., Williams, D., 2011. Contribution of glacier meltwater to streamflow in the
 794 Wind River Range, Wyoming, inferred via a Bayesian mixing model applied to isotopic
 795 measurements. *Hydrol. Process.*, 25(14), 2228–2236, doi:10.1002/hyp.7982, 2011.
 796

797 Chiogna, G., Santoni, E., Camin, F., Tonon, A., Majone, B., Trenti, A., Bellin, A., 2014. Stable
 798 isotope characterization of the Vermigliana catchment, *J. Hydrol.*, 509, 295–305.
 799 doi:10.1016/j.jhydrol.2013.11.052, 2014.
 800

801 Craig, R., 1961. Isotopic variations in meteoric waters. *Science* 133, 1702–1703.
 802

803 Cui, J., An, S., Wang, Z., Fang, C., Liu, Y., Yang, H., 2009. Using deuterium excess to determine
 804 the sources of high-altitude precipitation : Implications in hydrological relations between sub-alpine
 805 forests and alpine meadows. *J. Hydrol.*, 373(1-2), 24–33, doi:10.1016/j.jhydrol.2009.04.005, 2009.
 806

807 Dahlke, H., Lyon, S., Jansson, P., 2013. Isotopic investigation of runoff generation in a glacierized
 808 catchment in northern Sweden. *Hydrol. Process.*, 28, 1035–1050, doi:10.1002/hyp.9668, 2014.
 809

Formatted: Italian (Italy)

810 Dalai, T.K., Bhattacharya, S. K., Krishnaswami, S.,2002. Stable isotopes in the source waters of the
811 Yamuna and its tributaries: seasonal and altitudinal variations and relation to major cations. Hydrol.
812 Process, 16, 3345–3364, doi:10.1002/hyp.1104, 2002.

813
814 Dansgaard, W., 1964. Stable isotopes in precipitation. Tellus 16, 436–468

815
816 Della Chiesa S., Bertoldi G., Niedrist, G., Obojes N., Endrizzi S., Albertson J.D., Wohlfahrt G.,
817 Hörtnagl L., Tappeiner U., 2014. Modelling changes in grassland hydrological cycling along an
818 elevational gradient in the Alps. Ecohydrology DOI: 10.1002/eco.1471 (in press).

819
820 Dietermann, N., Weiler, M., 2013. Spatial distribution of stable water isotopes in alpine snow cover.
821 Hydrology and Earth System Sciences 17, 2657–2668. doi:10.5194/hess-17-2657-2013

822
823 Earman, S., Campbell, A. 2006. Isotopic exchange between snow and atmospheric water vapor:
824 Estimation of the snowmelt component of groundwater recharge in the southwestern United States.
825 J. Geophys., 111, 1–18, doi:10.1029/2005JD006470, 2006.

826
827 ~~Froehlich, K., Kralik, M., Papesch, W., Rank, D., Scheifinger, H., Stichler, W., 2008. Deuterium~~
828 ~~excess in precipitation of Alpine regions — moisture recycling. Isotopes in Environmental and Health~~
829 ~~Studies, Vol. 44, 1, 61–70.~~

830
831 Galos. S., Kaser G., 2014. The Mass Balance of Matscherferner 2012/13. University of Innsbruck,
832 project report.

833
834 Gat, J. R., Carmi, I. 1970. Evolution of the isotopic composition of atmospheric waters in the
835 Mediterranean Sea area. J. Geophys. Res.75: 3039–3048

836
837 Genereux D., 1998. Quantifying uncertainty in tracer-based hydrograph separations. Water Resources
838 Research, 34(4), 915–919, doi:10.1029/98WR00010.

839
840 Gonfiantini, R., Roche, M., Olivry, J., 2001. The altitude effect on the isotopic composition of tropical
841 rains. Chem. Geol., 181, 1–4, 147–167, doi: 10.1016/S0009-2541(01)00279-0

Formatted: Indent: First line: 0 cm, Line spacing: 1.5 lines

Formatted: English (United Kingdom)

Formatted: English (United Kingdom)

Field Code Changed

843 Gooseff, M. N., Lyons, W., McKnight, D. M., Vaughn, B. H., Fountain, A. G., & Dowling, C. (2006).
 844 A stable isotopic investigation of a polar desert hydrologic system, McMurdo dry valleys, Antarctica.
 845 Arctic, Antarctic, And Alpine Research, 38(1), 60-71.
 846

847 Grah, O., Beaulieu, J., 2013. The effect of climate change on glacier ablation and baseflow support
 848 in the Nooksack River basin and implications on Pacific salmonid species protection and recovery.
 849 Clim. Change, 120(3), 657–670, doi:10.1007/s10584-013-0747-y, 2013.
 850

851 Hughes, C. E., Crawford, J., 2013. Spatial and temporal variation in precipitation isotopes in the
 852 Sydney Basin, Australia. J. Hydrol., 489, 42–55, doi:10.1016/j.jhydrol.2013.02.036, 2013.
 853

854 Jeelani, G., Bhat, N. A., Shivanna, K., 2010. Use of $\delta^{18}\text{O}$ tracer to identify stream and spring
 855 origins of a mountainous catchment: A case study from Liddar watershed, Western Himalaya, India.
 856 J. Hydrol., 393(3-4), 257–264, doi:10.1016/j.jhydrol.2010.08.021, 2010.
 857

858 Jeelani, G., Kumar, U. S., Kumar, B., 2013. Variation of $\delta^{18}\text{O}$ and dD in precipitation and stream
 859 waters across the Kashmir Himalaya (India) to distinguish and estimate the seasonal sources of
 860 stream flow. J. Hydrol., 481, 157–165, doi:10.1016/j.jhydrol.2012.12.035, 2013.
 861

862 ~~Jin, L., Siegel, D. I., Lautz, L. K., Lu, Z., 2012. Identifying streamflow sources during spring~~
 863 ~~snowmelt using water chemistry and isotopic composition in semi arid mountain streams. J.~~
 864 ~~Hydrol., 470–471, 289–301, doi:10.1016/j.jhydrol.2012.09.009, 2012.~~
 865

866 Jost, G., Moore, R. D., Menounos, B., Wheate, R. 2012. Quantifying the contribution of glacier
 867 runoff to streamflow in the upper Columbia River Basin, Canada. Hydrol. Earth Syst. Sci., 16(3),
 868 849–860, doi:10.5194/hess-16-849-2012, 2012.
 869

870 Kääb A., Chiarle M., Raup B., ~~and~~ Schneider, C. ~~(2007.)~~ Climate change impacts on mountain
 871 glaciers and permafrost. Global and Planetary Change 56(1-2), p. vii-ix, DOI:
 872 10.1016/j.gloplacha.2006.07.008
 873

874 Knoll, C., 2010. A glacier inventory for South Tyrol, Italy, based on airborne laser-scanner data.
 875 Ann. Glaciol. 50 (53), 46–52.
 876

Formatted: English (United Kingdom)

877 Koboltschnig, G. R., Schöner, W., 2011. The relevance of glacier melt in the water cycle of the Alps:
 878 the example of Austria. *Hydrology and Earth System Sciences*, 15(6), 2039–2048. doi:10.5194/hess-
 879 15-2039-2011
 880

881 Kriegel, D., Mayer, C., Hagg, W., Vorogushyn, S., Duethmann, D., Gafurov, A., Farinotti, D., 2013.
 882 Changes in glacierisation, climate and runoff in the second half of the 20th century in the Naryn basin,
 883 Central Asia. *Global and Planetary Change*, 110, Part A, 51-61, 10.1016/j.gloplacha.2013.05.014.
 884

885 Kumar, U. S., Kumar, B., Rai, S. P., Sharma, S., 2010. Stable isotope ratios in precipitation and
 886 their relationship with meteorological conditions in the Kumaon Himalayas , India. *J. Hydrol.*,
 887 391(1-2), 1–8, doi:10.1016/j.jhydrol.2010.06.019, 2010.
 888

889 Lambs, L., 2000. Correlation of conductivity and stable isotope ^{18}O for the assessment of water
 890 origin in river system. *Chem. Geol.*, 164, 161–170
 891

892 Lee, J., Feng, X., Faiia, A. M., Posmentier, E. S., Kirchner, J. W., Osterhuber, R., Taylor, S., 2009.
 893 Isotopic evolution of a seasonal snowcover and its melt by isotopic exchange between liquid water
 894 and ice. *Chem. Geol.*, 270(1-4), 126–134, doi:10.1016/j.chemgeo.2009.11.011, 2010.
 895

896 Longinelli, A., Anglesio, E., Flora, O., 2006. Isotopic composition of precipitation in Northern
 897 Italy: reverse effect of anomalous climatic events. *J. Hydrol.*, 329, 471–476,
 898 doi:10.1016/j.jhydrol.2006.03.002, 2006.
 899

900 Longinelli, A., Selmo, E., 2003. Isotopic composition of precipitation in Italy: a first overall map. *J.*
 901 *Hydrol.*, 270, 75–88
 902

903 Longinelli, A., Stenni, B., Genoni, L., 2008. A stable isotope study of the Garda Lake, northern
 904 Italy: Its hydrological balance. *J. Hydrol.*, 360, 103–116, doi:10.1016/j.jhydrol.2008.07.020, 2008.
 905

906 Machavaram, M. and Whittemore, D.: Precipitation induced stream flow: An event based chemical
 907 and isotopic study of a small stream in the Great Plains region of the USA, *J. Hydrol.*, 470–480,
 908 doi:10.1016/j.jhydrol.2006.04.004, 2006.
 909

910 Mair, E., Bertoldi, G., Leitinger, G., Della Chiesa, S., Niedrist, G., and Tappeiner, U., 2013. ESOLIP
911 – estimate of solid and liquid precipitation at sub-daily time resolution by combining snow height and
912 rain gauge measurements. Hydrol. Earth Syst. Sci. Discuss., 10, 8683–8714, doi:10.5194/hessd-10-
913 8683-2013, 2013.

Formatted: Font: (Default) Times New Roman, 12 pt

914
915 Mao, L., Dell’Agnese, A., Huincache, C., Penna, D., Engel, M., Niedrist, G., Comiti, F., 2014.
916 Bedload hysteresis in a glacier-fed mountain river: bedload hysteresis in a glacier-fed mountain river.
917 Earth Surf. Proc. Land., 39, 964–976. doi:10.1002/esp.3563

Formatted: Italian (Italy)

Formatted: Justified, Indent: First line: 0 cm, Line spacing:
1.5 lines

918
919 Maurya, A. S., Shah, M., Deshpande, R. D., Bhardwaj, R. M., Prasad, A., Gupta, S. K., 2011.
920 Hydrograph separation and precipitation source identification using stable water isotopes and
921 conductivity: River Ganga at Himalayan foothills. Hydrol. Process., 25(10), 1521–1530,
922 doi:10.1002/hyp.7912, 2011.

923
924 Meriano, M., Howard, K. W. F., Eyles, N., 2011. The role of midsummer urban aquifer recharge in
925 stormflow generation using isotopic and chemical hydrograph separation techniques. J. Hydrol.,
926 396(1-2), 82–93, doi:10.1016/j.jhydrol.2010.10.041, 2011.

927
928 Milner, A., Brown, L., Hannah, D., 2009. Hydroecological response of river systems to shrinking
929 glaciers. Hydrol. Process., 77, 62–77, doi: 10.1002/hyp.7197

930
931 Molini, A., Katul, G. G., Porporato, A., 2011. Maximum discharge from snowmelt in a changing
932 climate. Geophysical Research Letters, 38(5), 1–5. doi:10.1029/2010GL046477

933
934 Neal, C., Reynolds, B., Kirchner, J. W., Rowland, P., Norris, D., Sleep, D., Lawlor, A., Woods, C.,
935 Thacker, S., Guyatt, H., Vincent, C., Lehto, K., Grant, S., Williams, J., Neal, M., Wickham, H.,
936 Harman, S. and Armstrong, L., 2013. High-frequency precipitation and stream water quality time
937 series from Plynlimon, Wales: an openly accessible data resource spanning the periodic table.
938 Hydrol. Process., 27, 2531–2539, doi:10.1002/hyp.9814, 2013.

939
940 Notarnicola C., Duguay M., Moelg N., Schellenberger T., Tetzlaff A., Monsorno R., Costa A., Steurer
941 C., Zebisch M., 2013. Snow Cover Maps from MODIS Images at 250 m Resolution, Part 1: Algorithm
942 Description. Remote Sensing 5(1): 110-126.

943

944 Ohlanders, N., Rodriguez, M., McPhee, J., 2013. Stable water isotope variation in a Central Andean
 945 watershed dominated by glacier and snowmelt. *Hydrol. Earth Syst. Sci.*, 17(3), 1035–1050,
 946 doi:10.5194/hess-17-1035-2013, 2013.
 947
 948 Pasolli L., Notarnicola C., Bertoldi G., Della Chiesa S., Niedrist G., Bruzzone L., Tappeiner U.,
 949 Zebisch M., 2014. Soil moisture monitoring in mountain areas by using high resolution SAR images:
 950 results from a feasibility study. *European Journal of Soil Science* 2014 (in press).
 951
 952 Pearce, A. J., Stewart, M. K., Sklash, M. G., 1986. Storm runoff generation in humid headwater
 953 catchments, 1, where does the water come from? *Water Resour Res* 22:1263–1271
 954
 955 Pellerin, B., Wollheim, W., 2008. The application of electrical conductivity as a tracer for
 956 hydrograph separation in urban catchments, *Hydrol. Process.*, 22, 1810–1818, doi:10.1002/hyp,
 957 2008.
 958
 959 Peng, H., Mayer, B., Harris, S., Krouse, H.R., 2004. A 10-year record of stable isotope ratios of
 960 hydrogen and oxygen in precipitation at Calgary, Alberta, Canada. *Tellus B* 56, 147–159
 961
 962 Penna, D., Mao, L., Comiti, F., Engel, M., Dell’Agnese, A., Bertoldi, G., 2013. Hydrological effects
 963 of glacier melt and snowmelt in a high-elevation catchment. *Die Bodenkultur*, 64 (3-4), 93-98.
 964
 965 Penna, D., Stenni, B., Šanda, M., Wrede, S., Bogaard, T. A., Gobbi, A., Borga, M., Fischer, B. M.
 966 C., Bonazza, M., Chárová, Z., 2010. On the reproducibility and repeatability of laser absorption
 967 spectroscopy measurements for $\delta^2\text{H}$ and $\delta^{18}\text{O}$ isotopic analysis. *Hydrol. Earth Syst. Sci. Discuss.*,
 968 7(3), 2975–3014, doi:10.5194/hessd-7-2975-2010, 2010.
 969
 970 Penna, D., Stenni, B., Šanda, M., Wrede, S., Bogaard, T. A., Michelini, M., Fischer, B. M. C.,
 971 Gobbi, a., Mantese, N., Zuecco, G., Borga, M., Bonazza, M., Sobotková, M., Čejková, B.,
 972 Wassenaar, L. I., 2012. Technical Note: Evaluation of between-sample memory effects in the
 973 analysis of $\delta^2\text{H}$ and $\delta^{18}\text{O}$ of water samples measured by laser spectrometers. *Hydrol. Earth Syst.*
 974 *Sci.*, 16(10), 3925–3933, doi:10.5194/hess-16-3925-2012, 2012.
 975

976 Poage, M.A., Chamberlain, C.P., 2001. Empirical relationships between elevation and the stable
977 isotope composition of precipitation and surface waters: considerations for studies of paleoelevation
978 change. *Am. J. Sci.* 301, 1–15.

979

980 [Racoviteanu, A.E., Armstrong, R., Williams, M.W., 2013. Evaluation of an ice ablation model to](#)
981 [estimate the contribution of melting glacier ice to annual discharge in the Nepal Himalaya: glacial](#)
982 [contributions to annual streamflow in Nepal Himalaya. *Water Resour. Res.*, 49, 5117–5133,](#)
983 [doi:10.1002/wrcr.20370](#)

984

985 Shanley, J., Kendall, C., 2002. Controls on old and new water contributions to stream flow at some
986 nested catchments in Vermont, USA. *Hydrol. Process.*, 16, 589–609, doi:10.1002/hyp.312, 2002.

987

988 Stewart, I., 2009. Changes in snowpack and snowmelt runoff for key mountain regions. *Hydrol.*
989 *Process.*, 94, 78–94, doi:10.1002/hyp, 2009.

990

991 Taylor, S., Feng, X., Kirchner, J. W., Osterhuber, R., Klaue, B., Renshaw, C. E., 2001. Isotopic
992 evolution of a seasonal snowpack and its melt. *Water Resour. Res.*, 37(3), 759–769,
993 doi:10.1029/2000WR900341, 2001.

994

995 Uhlmann, B., 2013. Modelling runoff in a Swiss glacierized catchment – Part II : daily discharge
996 and glacier evolution in the Findelen basin. *Int. J. Climatol.*, 1307(June 2012), 33, 1301–1307,
997 doi:10.1002/joc.3516, 2013.

998

999 Wassenaar, L. I., Athanasopoulos, P., Hendry, M. J., 2013. Isotope hydrology of precipitation ,
1000 surface and ground waters in the Okanagan Valley , British Columbia , Canada. *J. Hydrol.*, 411(1-
1001 2), 37–48, doi:10.1016/j.jhydrol.2011.09.032, 2011.

1002

1003 Windhorst, D., Waltz, T., 2013. Impact of elevation and weather patterns on the isotopic
1004 composition of precipitation in a tropical montane rainforest. *Hydrol. Earth Syst. Sci.*, 409–419,
1005 doi:10.5194/hess-17-409-2013, 2013.

1006

1007 Yang, Y., Xiao, H., Wei, Y., Zhao, L., Zou, S., Yang, Q., Yin, Z., 2012. Hydrological processes in
1008 the different landscape zones of alpine cold regions in the wet season, combining isotopic and
1009 hydrochemical tracers. *Hydrol. Process.*, 26(10), 1457–1466, doi:10.1002/hyp.8275, 2012.

1010

1011 Yde, J. C., Tvis Knudsen, N. The importance of oxygen isotope provenance in relation to solute
1012 content of bulk meltwaters at Imersuaq Glacier, West Greenland. *Hydrol. Process.*, 18(1), 125–139,
1013 doi:10.1002/hyp.1317, 2004.

1014

1015 Zabaleta, A., Antigüedad, I., 2013. Streamflow response of a small forested catchment on different
1016 timescales. *Hydrol. Earth Syst. Sci.*, 211–223, doi:10.5194/hess-17-211-2013, 2013.

1017

1018 Zhang, Y. H., Song, X. F., Wu, Y. Q., 2009. Use of oxygen-18 isotope to quantify flows in the upriver
1019 and middle reaches of the Heihe River, Northwestern China, *Environ. Geol.*, 58(3), 645–653,
1020 doi:10.1007/s00254-008-1539-y, 2009.

1021

1022 Zhou, S., Wang, Z., Joswiak, D.R., 2014. From precipitation to runoff: stable isotopic fractionation
1023 effect of glacier melting on a catchment scale: catchment-scale isotopic fractionation effect of
1024 glacier melting. *Hydrol. Process.*, 28, 3341–3349, doi:10.1002/hyp.9911

1025

1026

1027 **Tables**

1028

1029 Table 1. Main morphometric properties of the sub-catchments considered in the study area.

1030 *: after the South Tyrolean Glacier Inventory (Knoll, 2010);

1031 **: after Boeckli et al. (2012).

1032

Sub-Catchment	Drainage area (km ²)	Glacierized area (%)*	Area with rock glacier (%)**	Elevation range (m a.s.l.)	Average slope (°)	Average aspect
S1	35.0	11.6	3.7	1809-3725	29.9	S
S2	27.4	14.9	3.2	2001-3725	31.8	S
S3-LSG	18.6	16.9	4.2	2151-3725	34.8	E
S4	15.4	20.4	4.4	2231-3725	32.3	S
S5-USG	11.2	26.1	4.9	2333-3725	30.8	S
S6	7.6	36.8	2.2	2401-3725	29.5	S
S7	7.5	37.3	2.3	2407-3725	29.5	S
S8	5.4	51.1	0.0	2415-3725	28.7	W
T1	10.2	0.0	3.6	1775-3280	31.5	S
T2-SG	17.5	0.9	0.2	2028-3316	19.7	W
T3	<0.0	0.0	0.0	2159-2434	30.4	W
T4	1.22	0.0	0.0	2232-3296	35.0	W
T5	1.8	2.2	9.4	2416-3460	30.7	S
total	61.7	6.6	3.5	1632-3725	31.8	S

1033

1034

1035 Table 2. Number of rainfall, stream and spring samples ~~collected during this study~~ and elevation of
1036 each sampling location. RF: rainfall; S: Saldur River; T: tributaries of the Saldur River; SPR: springs.
1037 ~~Note that s~~Samples ~~from at~~ RF1 and RF5 were not collected in 2011. Samples ~~at from~~ T1 were
1038 collected only in 2012, and samples ~~at from~~ T3 only in 2011. In 2013 no tributaries were sampled and
1039 samples from the main stream were collected only at four locations (S1, S3-LSG, S5-LSG, S8). Note
1040 that S7 is the confluence just downstream S8 and T5 but after a large flood event occurred on
1041 September 4th, 2011 that modified the morphology of the upper part of the Saldur River, it was moved
1042 to S6.

1043

Sampling location	Elevation (m a.s.l.)	Number of samples
RF1	1575	12
RF2	1829	16
RF3	2154	15
RF4	2336	15
RF5	2575	8
S1	1809	66
S2	2001	32
S3-LSG	2150	89
S4	2231	20
S5-USG	2333	27
S6	2401	8
S7	2410	9
S8	2415	23
T1	1775	13
T2-SG	2027	32
T3	2159	18
T4	2242	21
T5	2415	18
SPR1	2360	15
SPR2	2348	16
SPR3	2342	16
SPR4	2334	25

1044

1045 Table 3. Local meteoric water lines (LMWL) found reported by different authors for mountain sites
1046 in Northern Italy.

Reference	Study area	LMWL
<u>Longinelli and Selmo (2003); Longinelli and Stenni (2008)</u>	<u>Across four regions in Northern Italy, between 400 and 2125 m a.s.l.</u>	$\delta^2H\text{ (‰)} = 7.7 \delta^{18}O + 9.4$
<u>Chiogna et al. (2014)</u>	<u>Vermigliana catchment, Northern Italy, at 1176 m a.s.l.</u>	$\delta^2H\text{ (‰)} = 7.6 \delta^{18}O + 2.7$
<u>Chiogna et al. (2014)</u>	<u>Vermigliana catchment, Northern Italy, at 2731 m a.s.l.</u>	$\delta^2H\text{ (‰)} = 8.0 \delta^{18}O + 7.8$

Formatted: English (United Kingdom)

Formatted: English (United Kingdom)

Formatted: English (United Kingdom)

1047

1048

1049

1050

1051

1052

1053

1054

1055

Table 34. Parameters of the linear relationship between $\delta^{18}\text{O}$ and $\delta^2\text{H}$ for ~~snow~~, snowmelt, ~~and~~ ice melt and snowpack samples presented in Fig. 4, and for all stream water (Saldur and tributaries) and groundwater samples.

	n	slope	intercept	R ²
Snowmelt (from spring and summer snow patches)	23	8.1	9.7	0.99
Snowmelt (from snowmelt samplers)	10	7.9	4.7	0.99
Ice melt (rivulets on the glacier surface)	16	7.7	7.8	0.98
Ice melt (melting debris-covered ice)	9	7.6	5.4	0.92
Winter snowpack	22	8.2	15.0	0.97
<u>Stream water (Saldur River)</u>	<u>274</u>	<u>7.9</u>	<u>9.5</u>	<u>0.92</u>
<u>Stream water (tributaries)</u>	<u>102</u>	<u>6.5</u>	<u>-10.5</u>	<u>0.92</u>
<u>Groundwater</u>	<u>72</u>	<u>7.2</u>	<u>-1.9</u>	<u>0.95</u>

Formatted: Line spacing: 1.5 lines

1056 Table 4. Parameters of the linear relationship between $\delta^{18}\text{O}$ and $\delta^2\text{H}$ for all stream water (Saldur and
1057 tributaries) and groundwater samples.

	n	slope	interecept	R ²
Stream water (Saldur River)	274	7.9	9.5	0.92
Stream water (tributaries)	102	6.5	-10.5	0.92
Groundwater	72	7.2	-1.9	0.95

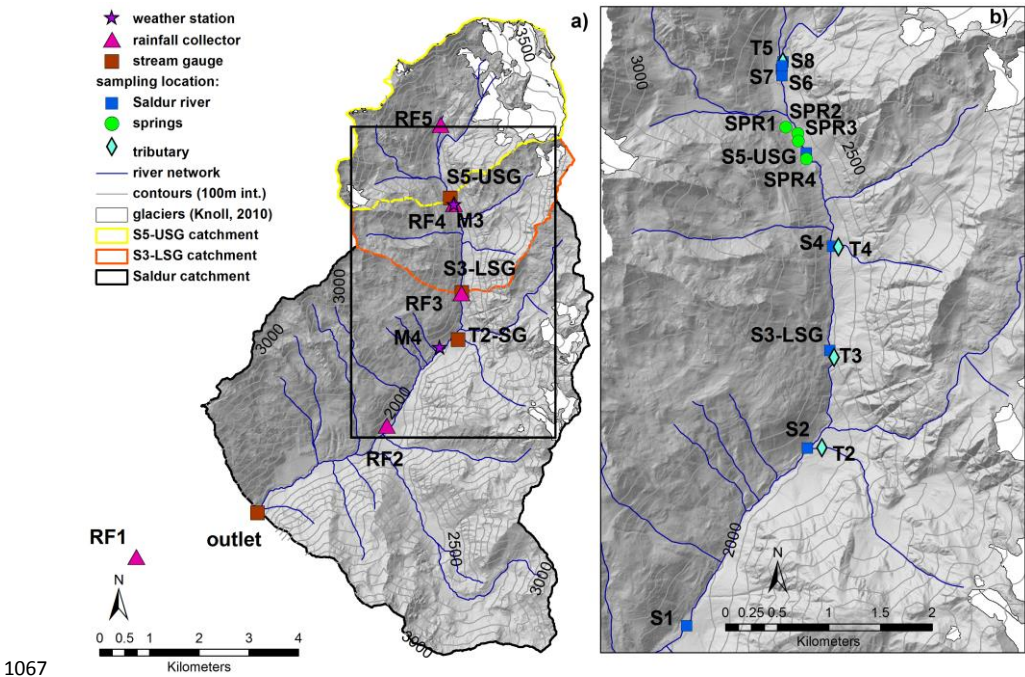
1059

1060 Table 5. Average (three years) snowmelt contribution to groundwater recharge based on $\delta^2\text{H}$ data.
1061 The \pm uncertainty at 70% ~~computed according to Genereux (1998)~~ is reported after each estimate.

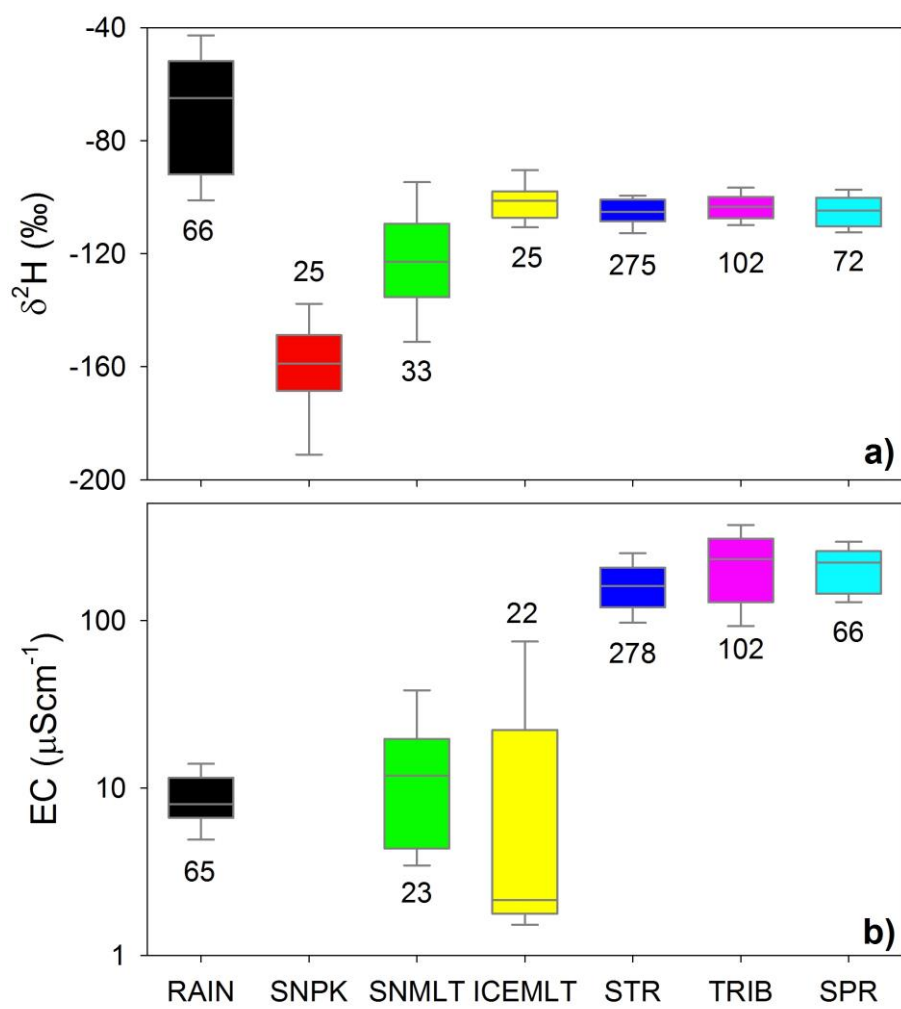
1062

	Snowmelt contribution (%)
SPR1	71 \pm 21 +6
SPR2	72 \pm 1 9 5
SPR3	70 \pm 21 +6
SPR4	58 \pm 24 +5

1063
1064



1067
1068 Fig. 1. Map of the Saldur catchment with position of the rainfall collectors, stream gauges and weather
1069 stations (panel a); zoom in showing the sampling locations for isotopic and EC analysis (panel b).



Formatted: Font: Times New Roman, 12 pt

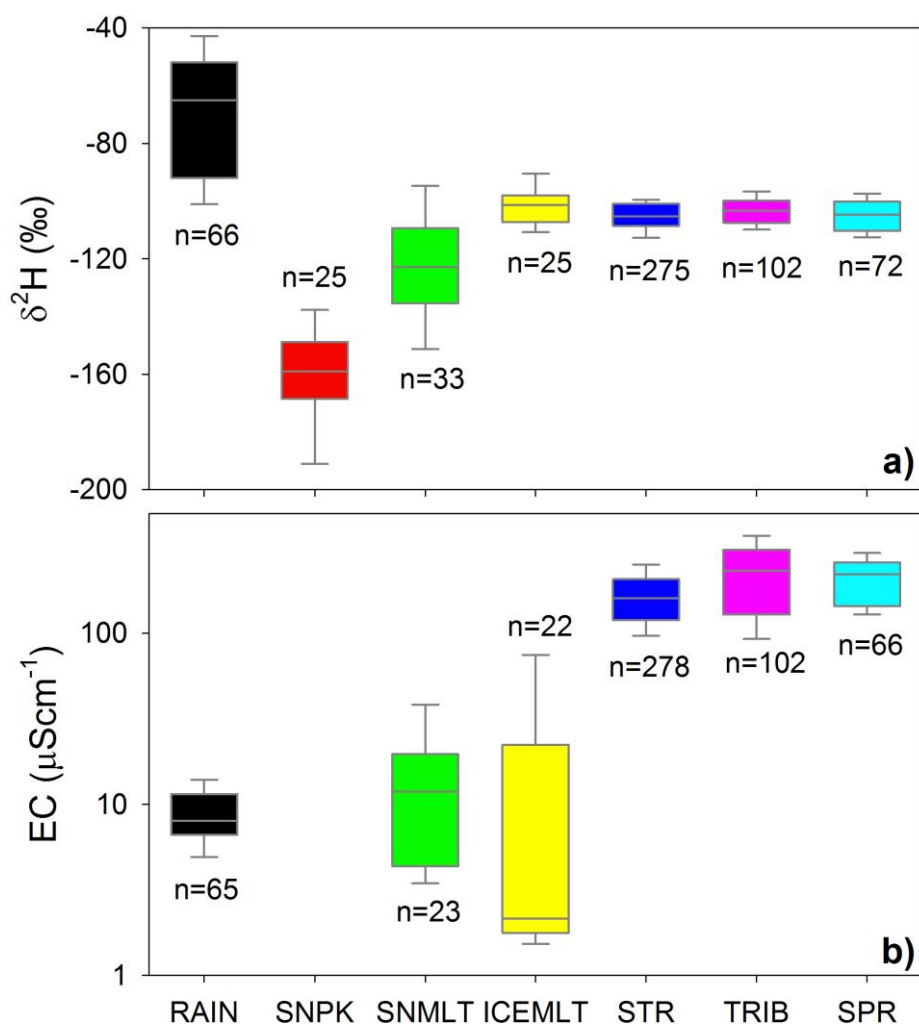


Fig. 2. Box-plot for $\delta^2\text{H}$ (panel a) and EC (panel b) of all water samples collected in this study. The whiskers represent the 10th and 90th percentiles, the box limits indicate the 25th and 75th percentiles and the line within the box marks the median. Legend: RAIN: rainfall; SNPK: winter snowpack and three samples of fresh snowfall; SNMLT: snowmelt (from patches of old snow and from snowmelt samplers); ICEMLT: ice melt (glacier melt and debris-covered ice); STR: main stream; TRIB: tributaries; SPR: springs. The numbers below or above each box represents the number of samples. EC data of the snowpack (SNPK) were not available.

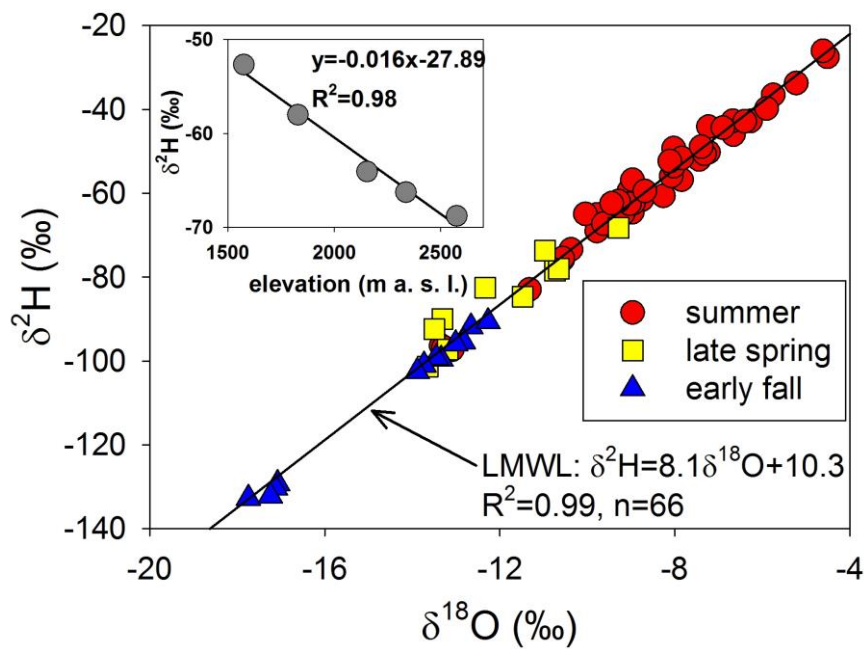
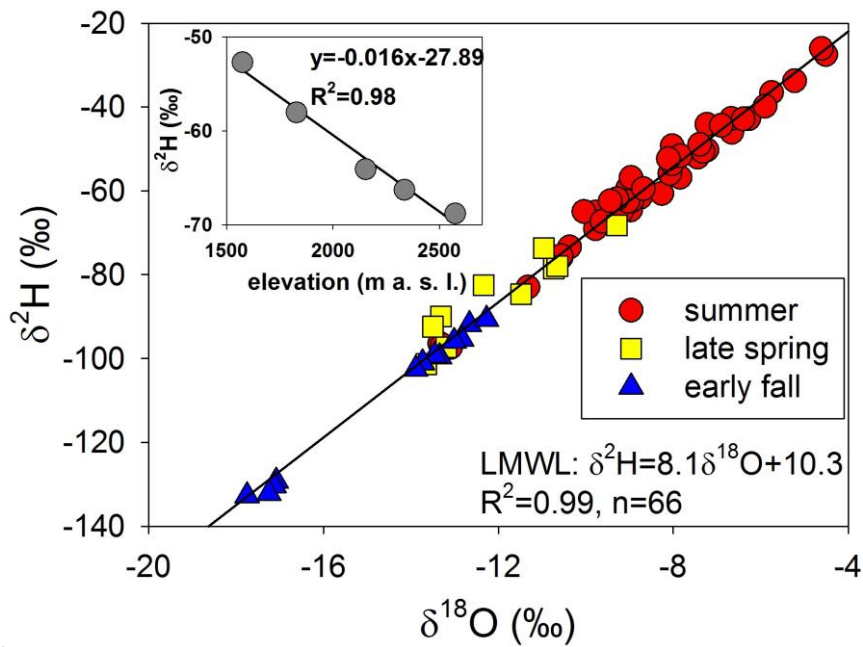
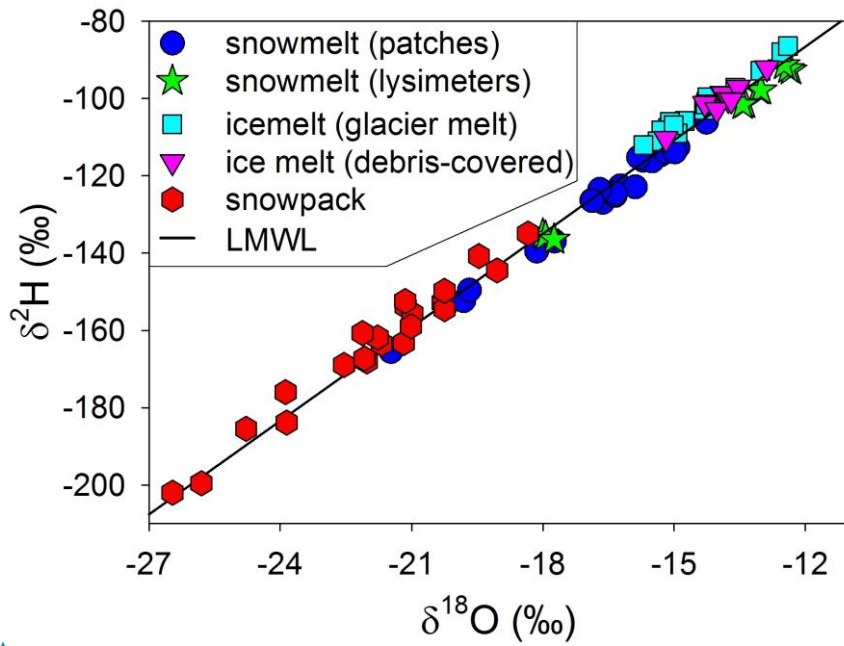


Fig. 3. Relationship between $\delta^{18}\text{O}$ and $\delta^2\text{H}$ values of rainfall samples ~~collected during the monitoring period in the Saldur catchment. In the inset: relation between elevation and~~ average (n=8) $\delta^2\text{H}$ in precipitation data ~~as a function of elevation offrom~~ the bulk rainfall collectors. For the inset plot, only data available for all five locations were averaged. Both correlations are statistically significant at 0.01 level.



Formatted: Font: Times New Roman, 12 pt

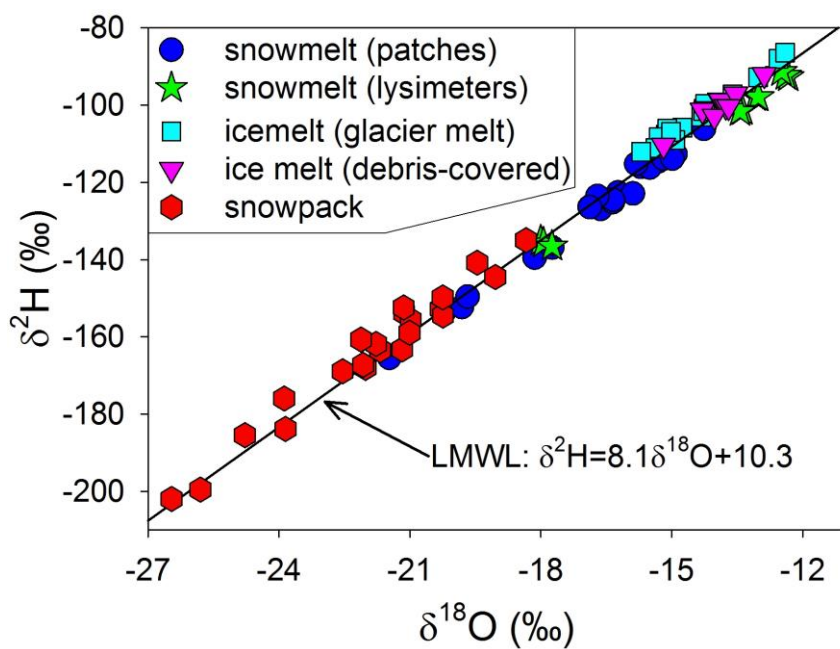
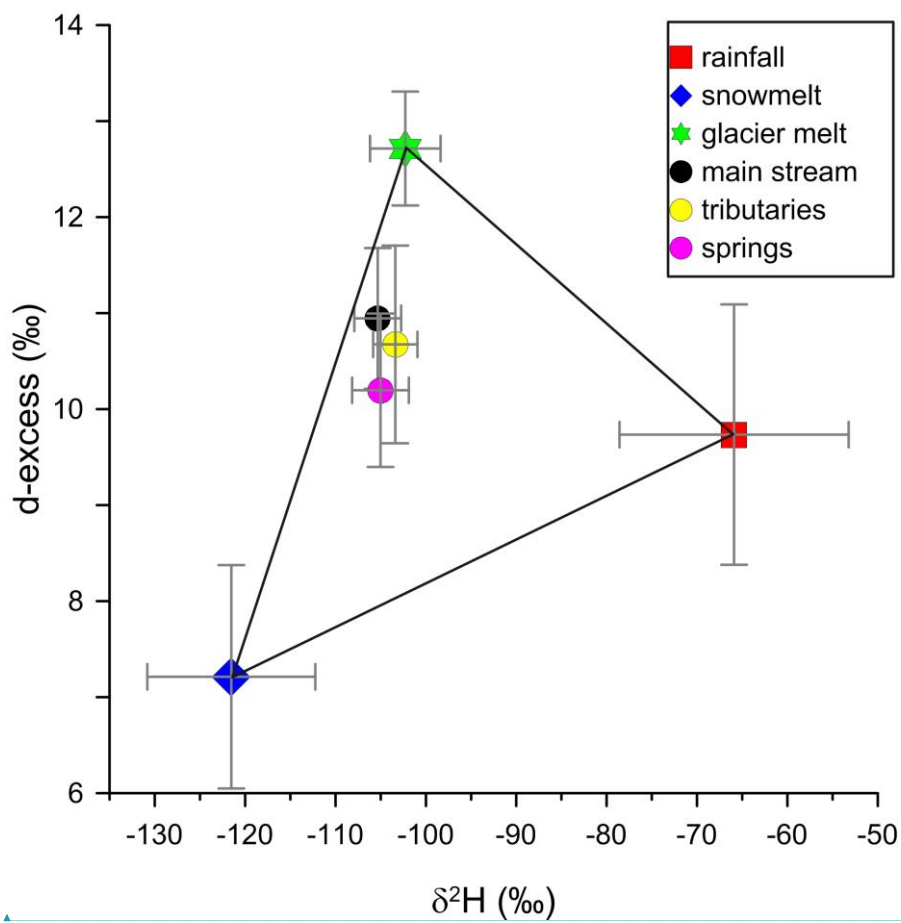


Fig. 4. Relationship between $\delta^2\text{H}$ and $\delta^{18}\text{O}$ values of snowmelt, ice melt and snow collected during the monitoring periods in the Saldur catchment.



Formatted: Font: Times New Roman, 12 pt

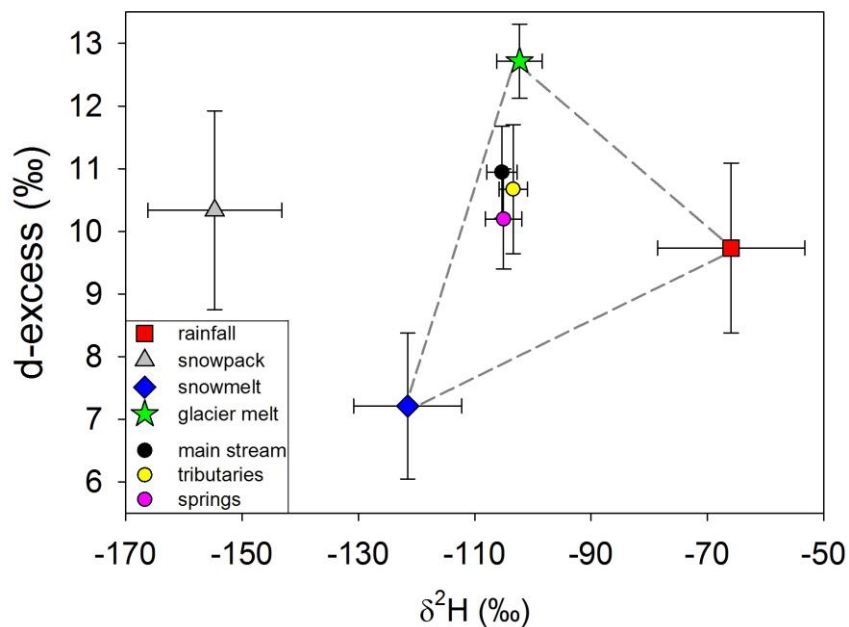


Fig. 5. Mixing diagram between $\delta^2\text{H}$ and d-excess including of all average values of samples collected from the main stream, the tributaries and the springs in the Saldur catchment. The error bars represent half of the standard deviation. Please note that the $\delta^2\text{H}$ and d-excess composition of rainwater samples was volume-weighted whereas the this was not possible for snow, snowmelt and glacier melt samples composition was not. The snowpack is excluded from the mixing space because it is not a direct hydrological input.

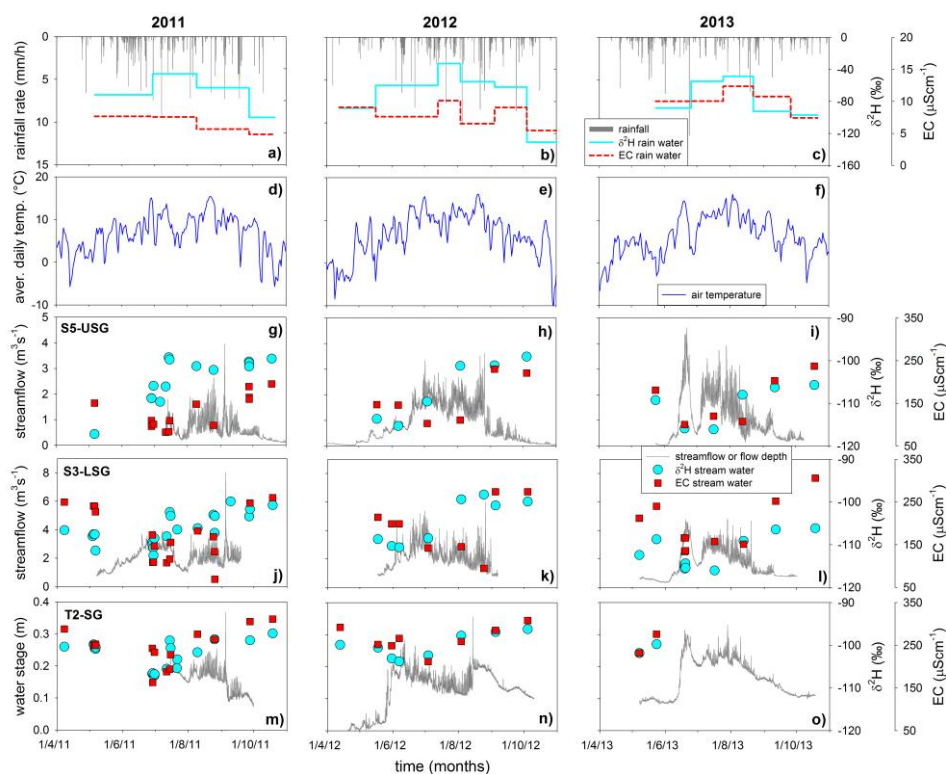


Fig. 6. Top row (panels a-c): hourly time series of precipitation (average of values from M3 and M4), and $\delta^2\text{H}$ and EC in bulk precipitation (average of values from RF2, RF3 and RF4). Second row (panels d-f): daily average temperature (average of values from M3 and M4). Middle row (panels g-i): hourly time series of streamflow at S5-USG, and $\delta^2\text{H}$ and EC of stream water. Fourth row (panels j-l): hourly time series of streamflow at S3-LSG, and $\delta^2\text{H}$ and EC of stream water. Bottom row (panels m-o): hourly time series of water height at T2-SG, and $\delta^2\text{H}$ and EC of stream water. On five occasions in 2011 multiple samples were taken within one day at S3-LSG; only samples taken in the morning, at peak flow and before sunset are shown in graphs j-l. At S3-LSG, on five occasions in 2011, multiple samples during the day were taken but, for the sake of clarity, only three samples collected at early morning (if available), approximately at peak flow and before sunset are shown. All panels refer to the period between April 1 and October 31, when the majority of water samples was collected.

Formatted: Font: (Default) Times New Roman, 12 pt

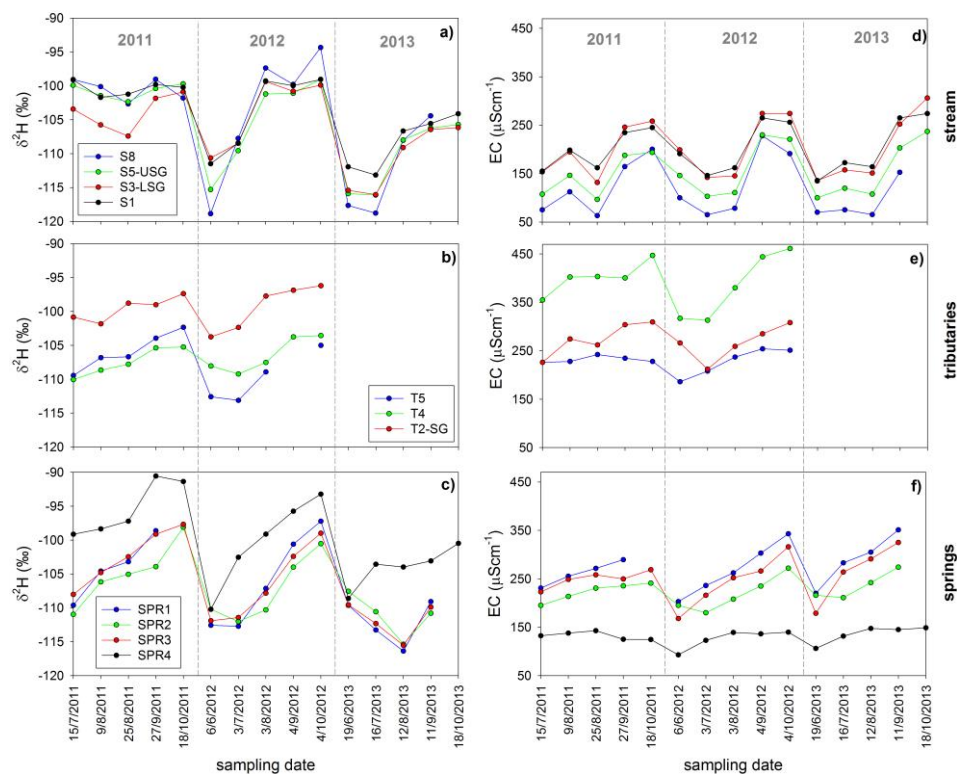
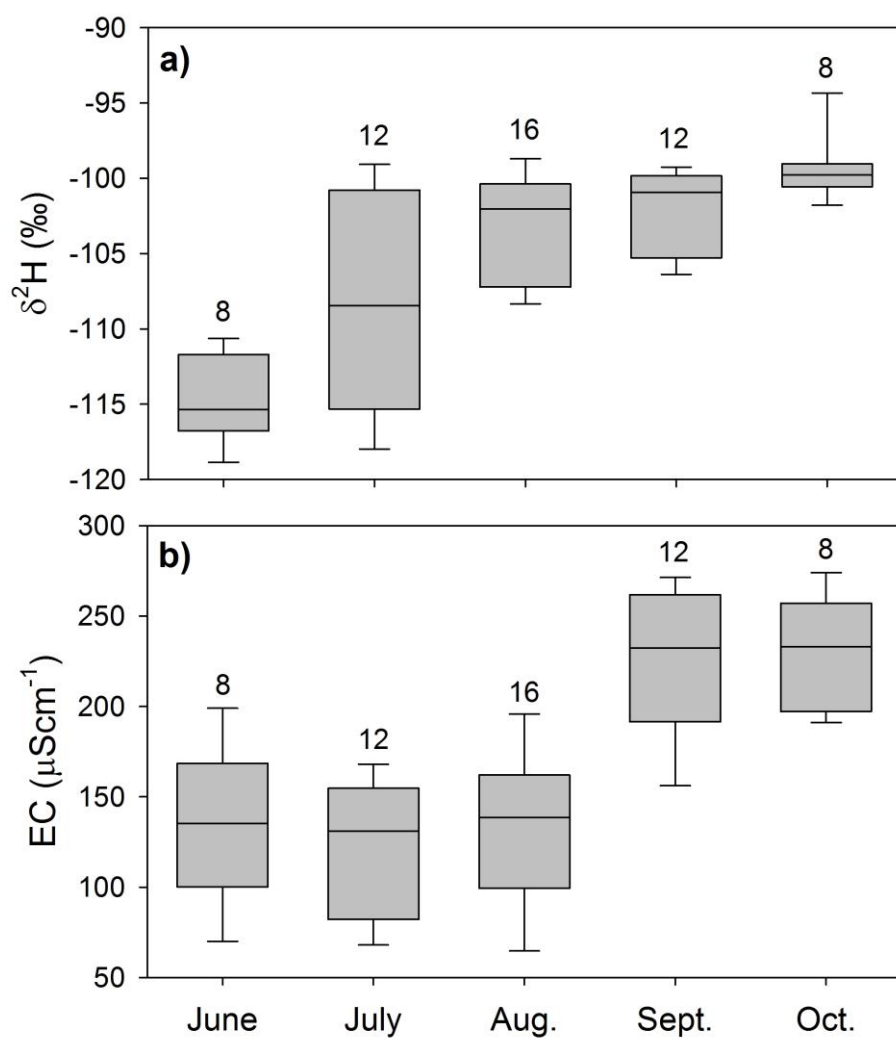


Fig. 7. Inter-annual variability of isotopic composition and EC of stream water and groundwater for the four locations in the Saldur River for which data were available for all three monitoring years (panels a and d); the three tributaries for which the most numerous measurements were available (panels b and e); and the four springs (panels c and f) for sampling days in 2011, 2012 and 2013. Note that the spacing on the x-axis is not proportional to the temporal distance between the sampling dates.



Formatted: Font: Times New Roman, 12 pt

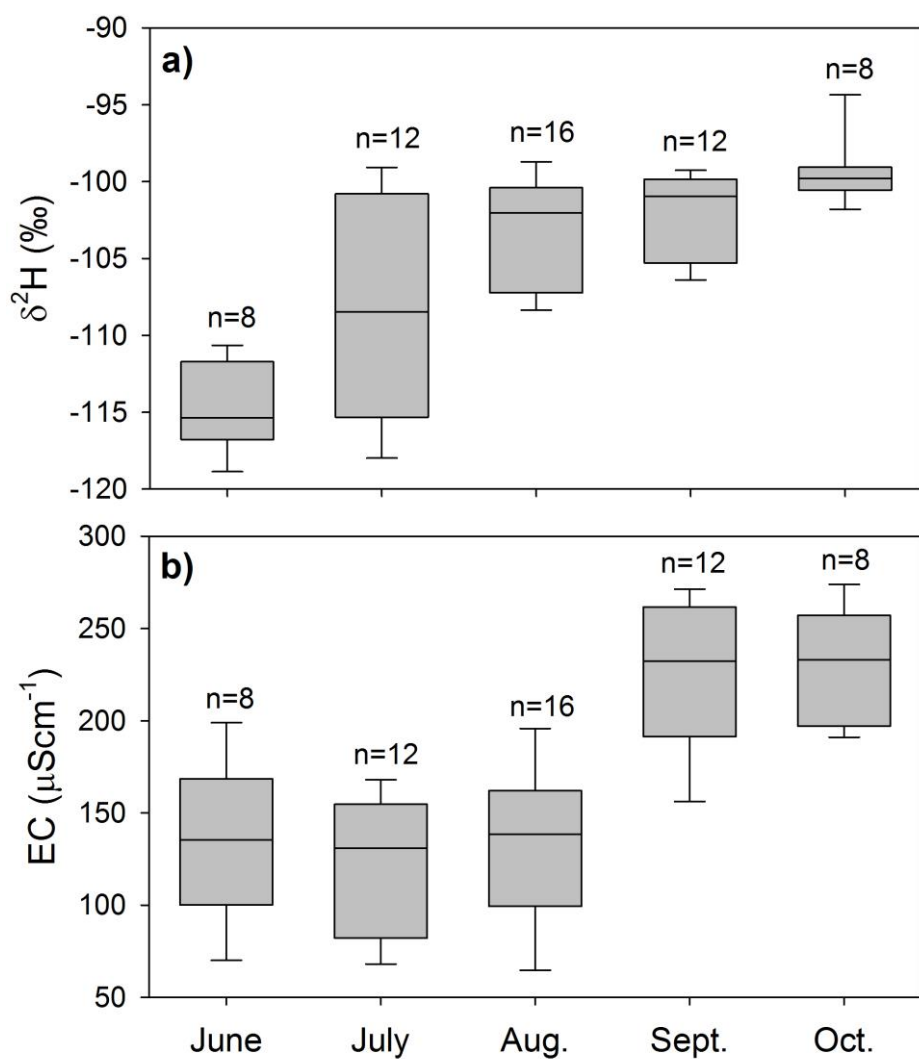
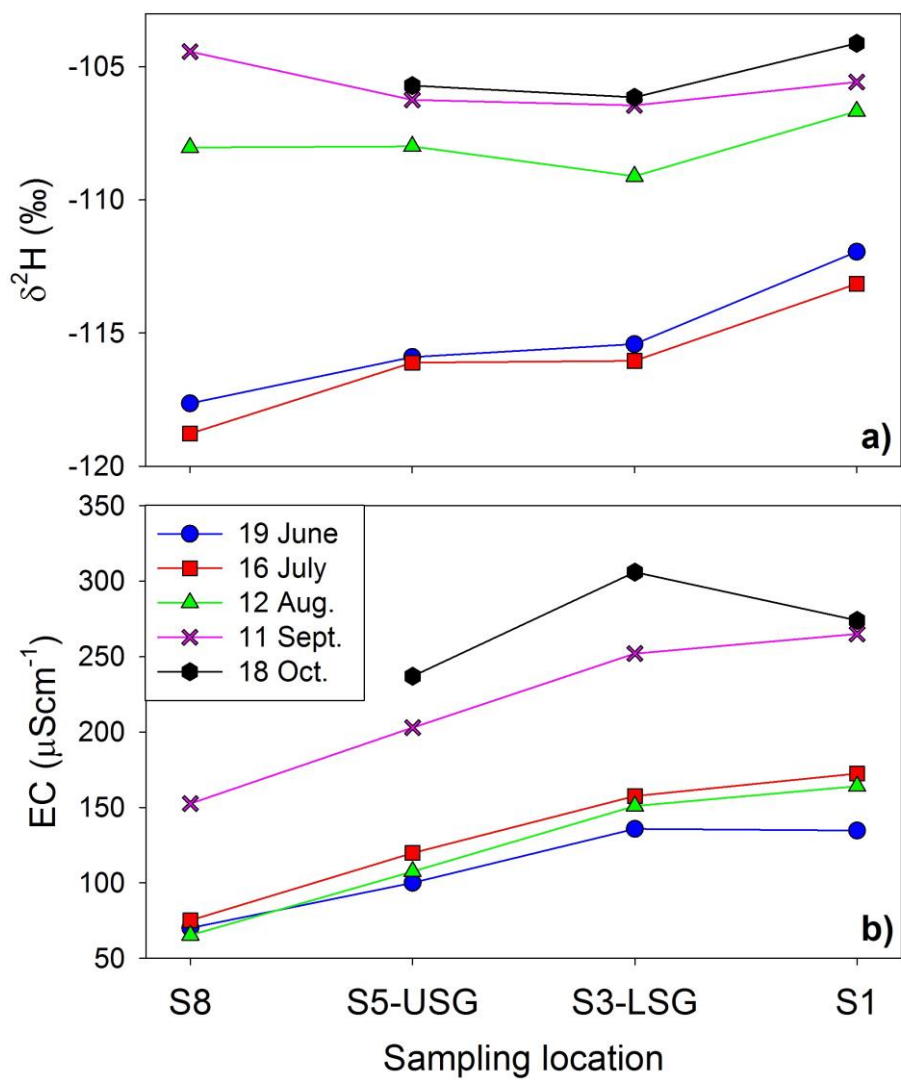


Fig. 8. Boxplot of $\delta^2\text{H}$ (panel a) and EC (panel b) of stream water data collected at the same time at the four selected locations along the Saldur River (S1, S3-LSG, S5 and S8) in 2011, 2012 and 2013 and grouped according to the sampling month. The whiskers represent the 10th and 90th percentiles, the box limits indicate the 25th and 75th percentiles and the line within the box marks the median.



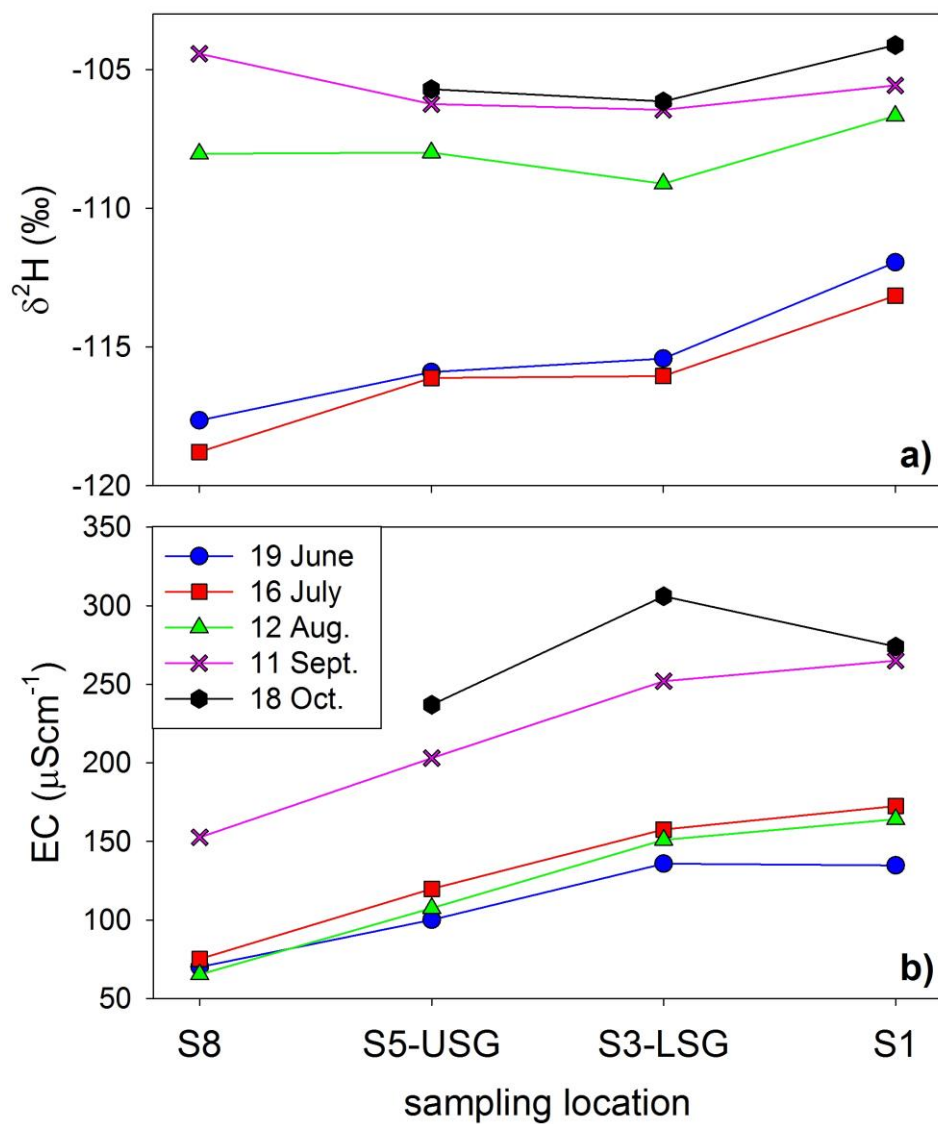


Fig. 9. Isotopic composition and EC of stream water ~~of-measured at~~ selected locations along the Saldur River for different sampling days during the 2013 monitoring year. Sampling started at 15:00 at S8 and ended approximately at 17:30 at S1. On October 18 it was not possible to sample location S8, sampling started at S5-USG and was carried out between 13:45 and 14:45.

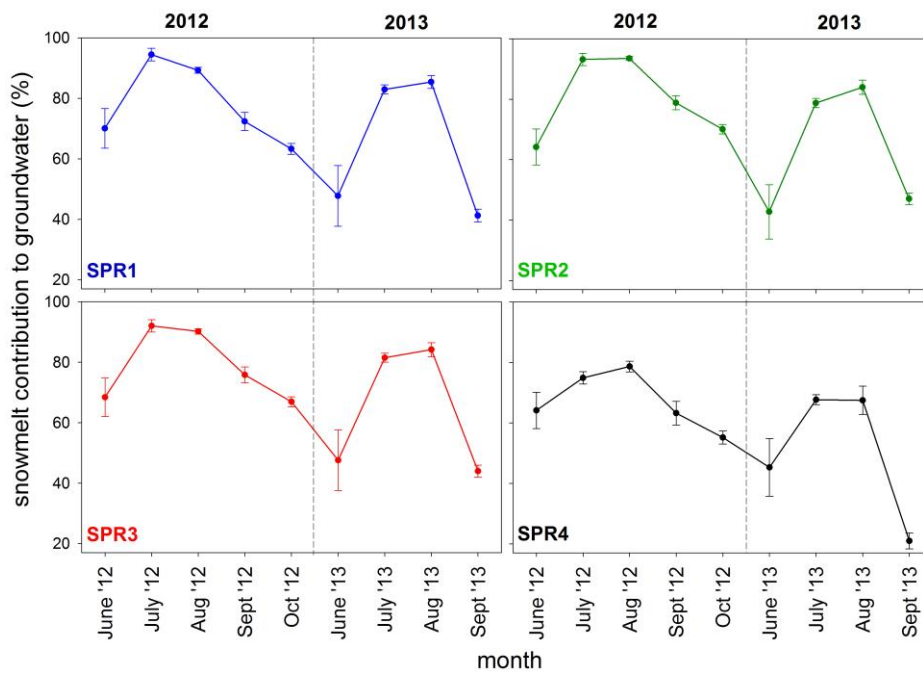


Fig. 10. Snowmelt contribution to groundwater recharge based on $\delta^2\text{H}$ data for different sampling times in 2012 and 2013. The error bars indicate the \pm uncertainty at 70%.